# MODELING THE EFFECTS OF PARTIAL THROUGHFALL EXCLUSION ON THE DISTRIBUTION OF SOIL WATER IN A BRAZILIAN OXISOL UNDER TROPICAL MOIST FOREST

by

ELIZABETH LESLIE BELK

(Under the Direction of Daniel Markewitz)

## ABSTRACT

Access to resource reserves in deep soil during periods of drought determines whether or not the tropical moist forests of Amazonia will be buffered from the deleterious effects of water deficit. Severe water stress may lead to tree mortality, changes in forest composition, and greater susceptibility to fire. A model was developed to simulate changes in the distribution of soil water within an existing throughfall exclusion experiment located in the Tapajós National Forest, east-central Amazonia (Brazil). Simulations using 2.5 years of data capture mild soil water depletion near the surface after the first treatment year, and decreasing soil moisture at depth during the second treatment year. Sensitivity analysis revealed that the model is sensitive to the parameters of the water retention and unsaturated flow equations. The model may be used to determine whether and how throughfall exclusion from a tropical rain forest affects water and nutrient cycling.

INDEX WORDS: Amazon, Modeling, Tropical moist forest, Oxisol, Soil water, Volumetric water content, Time Domain Reflectometry, Steady water flux, Drought, El Nino, Climate Change

# MODELING THE EFFECTS OF PARTIAL THROUGHFALL EXCLUSION ON THE DISTRIBUTION OF SOIL WATER IN A BRAZILIAN OXISOL UNDER TROPICAL MOIST FOREST

by

ELIZABETH LESLIE BELK

B.A., Vassar College, 1995

A Thesis Submitted to the Graduate Faculty of The University of Georgia in Partial Fulfillment of the Requirements for the Degree

MASTER OF SCIENCE

ATHENS, GEORGIA

2002

# MODELING THE EFFECTS OF PARTIAL THROUGHFALL EXCLUSION ON THE DISTRIBUTION OF SOIL WATER IN A BRAZILIAN OXISOL UNDER TROPICAL MOIST FOREST

by

ELIZABETH LESLIE BELK

Major Professor: Daniel Markewitz

Committee: Todd Rasmussen
David Radcliffe

Electronic Version Approved:

Maureen Grasso
Dean of the Graduate School
The University of Georgia
December 2002

## ACKNOWLEDGEMENTS

Many people deserve and have my gratitude for their assistance in the preparation of this thesis. Thank you to my major professor, Daniel Markewitz, for leaving his door open and making sure that I would find encouragement and guidance on the other side. I wish to thank the other members of my committee, Todd Rasmussen and David Radcliffe, both of whom were always willing to answer questions and share their far more extensive knowledge of hydrology and soil physics. Miguel Cabrera and John Dowd offered constructive advice on modeling and data issues. I would also like to thank Eric Davidson and Daniel Nepstad for their many contributions. Thank you to the members of the Woods Hole Research Center, the Empresa Brasileira de Pesquisa Agropecuaria-Belém Soils Lab and the Instituto de Pesquisa Ambiental da Amazonia for permitting me to use data and for providing much logistical support. In particular, I am grateful to David Ray, Karen Schwalbe, and Paul Lefebvre for facilitating communication and data transfers with the other researchers of the project. I would also like to thank the IPAM field crew for their faithful data collection, which made this project possible. Lastly, thank you to my family and friends for the love and support that so enrich my life.

## TABLE OF CONTENTS

Page

## LIST OF TABLES

Page

## LIST OF FIGURES

Page

# CHAPTER 1

# INTRODUCTION

Although tropical rain forests cover less than ten percent of the earth's land surface (Whittaker and Likens 1973), they have a disproportionate importance in the exchange of carbon, water, and energy between the biosphere and atmosphere (Schlesinger 1997). It has been estimated that the tropics account for at least 40% of global annual net primary productivity and evapotranspiration (Vitousek and Matson 1992). Almost half of the earth's intact tropical evergreen forest is located in the Amazon River basin (Williams et al. 1998). This region represents the largest remaining area of continuous tropical forest (Skole and Tucker 1993). While the function of the Amazon river basin in the global water cycle is well recognized, we are only beginning to understand the interaction of factors affecting the below-ground partitioning and availability of water and nutrients to vegetation in its forest ecosystems. These processes are important for interpreting how moist tropical forests manage to maintain evergreen canopies during the annual dry season and for predicting how these forests might respond to prolonged periods of drought, such as those that result from El Niño Southern Oscillation (ENSO) events.

To study the response of a moist Amazon forest to severe drought, a partial throughfall exclusion study was initiated in 1998 in the Tapajós National Forest, east-central Amazonia, Brazil (Nepstad et al. 2002). This experiment compares two one-

hectare plots, one of which receives natural rainfall, while the other has plastic panels installed in the forest understory during the rainy season. These panels capture approximately 60% of incoming throughfall, channeling the water to a system of gutters and diverting it from the soil. Both plots are surrounded by a 1.5-meter deep trench, which reduces the ability of the trees under study to access water from outside the plots (Sternberg et al. 2002). A variety of processes are being monitored, including: tree growth and mortality, sapflow, litterfall, leaf area index, forest floor decomposition, soil respiration, trace gas emissions, forest floor flammability, and the amounts and chemistry of precipitation, throughfall, litter leachate, and soil solutions. Soil moisture content is also measured by time domain reflectometry using soil shafts that allow access to twelve-meters depth in both the exclusion and control plots.

The overall objective of the throughfall exclusion experiment is to understand how tropical forests respond to severe drought. The goal of this project is to provide a physically based model of the soil water dynamics for the study site. Soil moisture measurements alone do not describe the magnitudes and rates of water fluxes because two layers may contain the same volume of water in a given volume of soil, but have different amounts of water flowing through them. A simulation model is proposed to predict whether and how soil water distribution, steady flux between layers, and deep drainage are affected by reduced inputs, in turn affecting the accessibility of water and nutrients to the forest. The throughfall exclusion experiment and its infrastructure provide an excellent opportunity to study soil water dynamics in deeply weathered tropical soils, and knowledge of the soil water dynamics will enhance the ability of investigators to explain other responses of the forest to drought conditions.

Understanding how the ecological functions of this tropical forest change during prolonged drought might illuminate the more subtle changes that occur during the annual dry season and help to predict the ability of these forests to tolerate reductions in precipitation associated with land use conversion or long-term climate change.

**References**

Nepstad, D.C., P. Moutinho, M. B. Dias-Filho, E. Davidson, G. Cardinot, D. Markewitz, R. Figueiredo, N. Vianna, J. Chambers, D. Ray, J. B. Guerreiros, P. Lefebvre, L. Sternberg, M. Moreira, L. Barros, F. Y. Ishida, I. Tohlver, E. Belk, K. Kalif and K. Schwalbe (2002). The effects of partial throughfall exclusion on canopy processes, aboveground production, and biogeochemistry of an Amazon forest. Journal of Geophysical Research 107(D20): 8085, doi: 10.1029/2001JD000360.

Schlesinger, W. H. (1997). Biogeochemistry: An Analysis of Global Change. Academic Press, New York. 588p.

Skole, D. and C. Tucker (1993). Tropical deforestation and habitat fragmentation in the Amazon: satellite data from 1978 to 1988. Science 260: 1905-1910.

Sternberg, L. da S. L., M. Z. Moreira and D. C. Nepstad (2002). Uptake of water by lateral roots of small trees in an Amazonian Tropical Forest. Plant and Soil 238: 151-158.

Vitousek, P. M. and P. A. Matson (1992). Tropical forests and trace gases: potential interactions between tropical biology and the atmospheric sciences. Biotropica 24(2): 233-239.

Whittaker, R. H. and G. E. Likens (1973). Carbon in the biota. Carbon and the Biosphere. G. M. Woodwell and E. V. Pecan. Washington, D.C., National Technical Information Service**:** 281-302.

Williams, M., Y. Malhi, A. D. Nobre, E. B. Rastetter, J. Grace and M.G. P. Pereira (1998). Seasonal variation in net carbon exchange and evapotranspiration in a Brazilian rain forest: a modelling analysis. Plant, Cell and Environment 21: 953-968.

# CHAPTER 2

# LITERATURE REVIEW

Amazon forests have a considerable impact on global cycles of elements, water, and energy. In this chapter, the general hydrology of the Amazon and interactions between climate and vegetation are reviewed. Evidence for ongoing and future reductions in precipitation driven by climate change, land use conversion, or other disturbances such as burning is also discussed. Estimates of the rainfall, throughfall, interception, and evapotranspiration components of the water cycle, especially those measured in evergreen Amazon forests similar to the one being modeled in this study, are provided. In addition, other factors that may influence soil water dynamics, such as soil hydraulic properties and rooting depth, are surveyed. The models of water flow, evapotranspiration, and plant uptake from which this model is descended are also reviewed.

## Amazon Climate and Hydrology

The hydrologic cycle of the Amazon River basin is unique. With the Andes Mountains forming a major barrier to the west, water enters the region carried primarily by easterly trade winds but also drains to the east by way of the Amazon River. This means that much of the water is directly recycled within the basin, especially over the central portion of the region (Salati and Vose 1984). There is a significant seasonality to rainfall in the Amazon, though the onset, duration, and relative difference between the

rainy and dry seasons will vary over the region and also from year to year (Morengo et al. 2001). The onset of the rainy season is generally earliest in central Brazil, where it starts around mid-October, and progresses northward so that the area north of the equator starts its rainy season around April. There is also a general east-west gradient in seasonality near the equator, with the rainy season arriving a little earlier toward the eastern portion of the basin. In addition to experiencing an annual dry season during which evapotranspiration may exceed rainfall, irregular oscillations in global climate patterns may also subject parts of the Amazon region to drier than normal conditions (Bruijnzeel 1996).

Although it has long been recognized that climate is an important factor determining the distribution of vegetation types, the interactions between land and atmosphere are numerous and complex. A feedback loop exists whereby climate may affect vegetation and vice versa (Shukla and Mintz 1982; Entekhabi et al. 1996). Regional hydrology is best understood in the context of this two-way interaction. The atmosphere converts water vapor to liquid that rains down to the soil, leaching nutrients from leaf surfaces along the way. The atmosphere also affects vegetation through changes in temperature, radiation, wind, and air humidity. In return, vegetation takes up water from the soil, converts it back into vapor and releases it to the atmosphere. In highly seasonal climates like the Amazon, this process appears to be a prerequisite for precipitation in the dry season. A numerical model of evapotranspiration and climate relationships found that when there was very little soil moisture at the beginning of the dry season, evapotranspiration was greatly inhibited, which let the atmospheric boundary

layer dry out and meant that the rest of the summer passed without rain (Shukla and Mintz 1982).

Soil moisture influences local climate via surface moisture and energy balances. For example, soil moisture availability affects albedo, which in turn affects the amount of solar radiation received at the ground. Radiative heating changes soil temperature, which impacts the soil thermal radiation and soil sensible heat flux (Entekhabi et al. 1996).

Given the importance of vegetative cover to water cycles, deforestation or other disurbances in the Amazon will likely lead to reductions in precipitation over the region (Nobre et al. 1991; Moreira et al. 1997). Another growing concern is that drought conditions associated with El Niño Southern Oscillation (ENSO) events appear to be increasing in frequency and severity (Nepstad et al. 2002). Although the exact consequence of these processes is still being studied and debated, all of them have the potential to alter the hydrologic cycle of the region.

Since the late 1970's, there has been a shift in ENSO events toward more El Niño warm phases and fewer, cooler La Niñas (Trenberth and Hoar 1996). A statistical analysis of drought trends based on air temperature and precipitation data from 1900-1995 concluded that climate change seems to be intensifying the hydrological response to ENSO (Dai et al. 1998).

El Niño Southern Oscillations occur about once every three to seven years and differ in magnitude and duration (Broecker 1996). Usually, equatorial trade winds push the Pacific Ocean surface water westward from South America and allow colder water to well up closer to the coast. During ENSO the trade winds are subdued or even change direction, which means that the ocean water cannot cool the air and reduce evaporation as

it normally does. This results in warming of the Pacific Ocean and triggers weather changes in South America and elsewhere around the globe (Dawson and O'Hare 2000).

Some studies have offered support for the theory that ENSO can cause weather anomalies in the Amazon basin and northeast of Brazil. Kousky et al. (1984) demonstrated that January to May precipitation was consistently below normal for stations scattered throughout the Amazon and northeast Brazil during each of the ENSO events of 1972, 1976, and 1983. Rogers (1988) studied the association of warm El Niño and cooler La Niña events with changes in precipitation and upper troposphere geopotential height anomalies over the Caribbean and tropical Americas. Geopotential heights are isopleths of constant atmospheric pressure. Atmospheric pressure decreases monotonically with distance from the earth's surface, but the rate of decrease with altitude depends on the mean density of air, so that geopotential heights are higher over warmer, less dense air. The difference in 12-month precipitation totals and in 200 millibar geopotential heights between warm and cool episodes were tested for statistical significance using two-tailed t-tests. The results of these analyses show significance at the 95% confidence intervals for an area including the northern portion of the Amazon. Ropelewski and Halpert (1987) also looked for relationships between regional patterns in precipitation and ENSO. Their analysis of monthly meteorological records from stations around the globe confirmed that ENSO affects rainfall, especially in the tropics. Seventeen regions where rainfall patterns were strongly associated with El Niño were identified around the globe (though there are potential relationships in other areas not included in the study due to insufficient data). One of these seventeen regions is located in northern South America, covering the northeast of Brazil and extending into the

Amazon. This area was found to have one of the strongest associations with El Niño, since rainfall was consistently below the average for 16 of 17 ENSO years studied. In fact, nine out of the eleven driest periods occurred during El Nino events.

Atmospheric general circulation models (AGCMs) attempting to quantify the hydrological and ecological consequences of land use conversion in the Amazon have generally predicted a rise in surface temperature (on the order of 0.4 – 2ºC) and a decrease in evapotranspiration (0.3 - 2.7 mm $day^{-1}$; Costa and Foley 2000). Most of the models also predict a decrease in precipitation (0.4 – 1.6 mm $day^{-1}$), though there are some models that do not (Lean et al. 1996). This discrepancy is largely due to uncertainties in soil parameters like infiltration (Delire et al. 1997) and vegetation albedo and roughness (Lean et al. 1996). Another complication is that specific types of land use change, such as logging, agriculture, or abandoned pasture may have different effects on hydrological processes, so the assumptions about the nature of land use conversion used in a model may alter their predictions of precipitation considerably (Bruijnzeel 1996).

Using a numerical model considering atmosphere-biosphere interactions, Shukla et al. (1990) simulated the effect of completely converting Amazon forest to pasture grass. Along with a 26% reduction in annual rainfall (642 mm), annual evapotranspiration declined by 30% (496 mm). The authors noted that these changes would hinder the re-establishment of forest vegetation upon pasture abandonment. According to simulations performed with The Center for Ocean-Land Atmosphere AGCM, deforestation to pasture or crop vegetation will alter the local climate toward hotter and drier conditions because water is not recycled back to the lower troposphere as efficiently as in the rainforest (Nobre et al. 1991). If a deforested area is large enough,

the impact could be region-wide. Since water vapor from Amazonia is what feeds into the central part of Brazil, the climate of that area would also be affected (Nobre et al. 1991).

An experiment using the National Center for Atmospheric Research GENESIS model predicted the future climate of the Amazon basin given additional conversion of forest to pasture and cropland along with rising ambient $CO_2$ concentrations (Costa and Foley 2000). Both of these trends are currently occurring and are expected to continue as the Amazon region continues to develop (Nobre et al. 1991; Bruijnzeel 1996). The results from GENESIS agreed with both previous simulation models and observational studies showing that total evapotranspiration decreases after deforestation. Transpiration declined proportionally more than evaporation. Precipitation also decreased, which is another common result of AGCM simulations. Annual temperature increased 1.4ºC. Within the model, a doubling of atmospheric $CO_2$ alone was predicted to increase precipitation. However, when both deforestation and doubled $CO_2$ were simulated together, deforestation dominated and the result was decreased precipitation overall. Both deforestation and $CO_2$ increased surface temperature so combining the two enhanced the response.

Lean et al. (1996) reported on the use of Anglo-Brazilian Amazonian Climate Observation Study (ABRACOS) vegetation and soil data to calibrate and validate the Hadley Centre model. The ABRACOS study was designed to collect field data from Amazon forests and pastures that could be used to parameterize and quality-check AGCMs (Gash et al. 1996). Several experiments were run, including simulations using parameter values for forest and pasture. To investigate the effect of albedo, roughness,

and infiltration, additional simulations were run in which it was assumed that all vegetation parameters would remain similar to forest values excepting the one parameter of interest. Increasing albedo from the forest to the pasture value decreased annual rainfall by 10% over northern South America. When only roughness was reduced to the pasture value, precipitation increased in parts of the basin. (The authors note that this result disagrees with earlier simulation experiments, and that the differences may be due to the degree to which roughness is changed and how the mountain barrier representing the Andes is modeled.) When it was assumed that conversion to pasture would be accompanied by surface soil compaction that lowers infiltration rates, evaporation decreased less than it did in the absence of compaction. Conflicting results on the effect of changes accompanying deforestation highlighted the need for field-based data to parameterize models.

Anthropogenic disturbances such as logging and conversion to pasture have been shown to alter the microclimate of forest in such a way as to make it more susceptible to fire (e.g. Uhl and Kauffman 1990). Thousands of square kilometers of primary Amazon forest burn every year, putting the forest at risk for recurrent fires (Cochrane and Schulze 1998). It has been previously observed that smoke from burning of biomass may inhibit rainfall. Analysis of the Tropical Rainfall Measuring Mission (TRMM) satellite data was able to establish that smoke releases cloud nuclei that make clouds more likely to develop droplets too small to condense into precipitation (Rosenfeld 1999). In addition to confirming the reduction in droplet size (from 14 to 9 micrometers), Kaufman and Fraser (1997) found that smoke increased cloud reflectance from 0.35 to 0.45. These effects occur even in deep tropical clouds (Rosenfeld 1999). Given the prospect of continued

burning of Amazon forest, smoke may have a significant impact on the basin's hydrology.

Any of the mechanisms discussed above has the potential to exaggerate the length and severity of seasonal drought in the Amazon by way of a direct effect on the introduction and partitioning of water in the forest. Studies reporting rainfall, throughfall, and interception characteristics will now be reviewed followed by estimates of evaporation and transpiration.

## Rainfall, Throughfall, and Interception

Rainfall in the Amazon region is highly variable in both space and time. Several studies have characterized average rainfall amounts for an Amazonian forest; the totals range from a little over 2000 mm up to 3000 mm per year (Chauvel et al. 1991; Leopoldo et al. 1995; Klinge et al. 2001). Meteorological records for sites in the east-central and central part of the region have documented a large interannual variability, with 878-2766 mm reported for Paragominas, Pará (1973-1994; Jipp et al. 1998) and 600-3000 mm reported for the Tapajós National Forest south of Santarém, Pará (Nepstad et al. 2002; Figure 2.1). The majority of precipitation occurs in an annual rainy season, which in the east-central area usually starts around December or January and lasts until June or July.

The vast majority of rain falling on a forest will come into direct contact with trees. Some of this water will travel down stems and trunks, or drip off leaves, on its way to the soil surface. These fractions are known as stemflow and throughfall, respectively. An additional, but usually significant fraction of intercepted water will evaporate directly from vegetative surfaces (Shuttleworth 1989). In the Amazon, stemflow estimates are


**Figure 2.1 Map of South America showing the extent of the Brazilian Amazon basin and the location of major cities.**

generally less than 2% of incoming rainfall, while throughfall is typically around 82-85% (e.g. Marin et al. 2000; Klinge et al. 2001). Interception rates as low as 8.9% have been measured (Llyod 1990).

Interception is usually determined indirectly by the difference between throughfall and gross rainfall. Estimates of interception vary widely, due in part to errors in measuring spatially heterogeneous throughfall amounts accurately. Shuttleworth (1989) discussed the techniques and errors associated with throughfall sampling. In comparing characteristics of temperate and tropical forests he notes that the high spatial variability of throughfall in tropical forests is what makes estimates of rainfall partitioning for a given storm prone to greater error. Throughfall is frequently concentrated in drip points, meaning that the number and placement of sample collectors can make a significant difference in estimates. For example, for five gauges in 10 random arrangements, a 10% error in the mean throughfall estimate would be expected. This error could be reduced to about 3.5% with 40 gauges in 30 random arrangements.

Interception is important because it represents water that recycles back to the atmosphere without reaching the soil. The portion of rainfall being intercepted will depend on the amount of water the canopy can hold, storm intensity and duration, the rate of evaporation, and the time between storms (Zeng et al. 2000). Tropical forests tend to have proportionally less interception loss than temperate ones because the larger, waxier leaves of the rainforest cannot hold as much water (Ubarana 1996). Low storage capacity means that tropical forest canopies saturate quickly. If too little time passes between storms, not all of the water stored in the canopy will have evaporated and there will be less interception from the subsequent storm. Rains of low intensity result in a higher

percentage of interception than do downpours and may not saturate the canopy completely before the storm ends (Zeng et al. 2000).

Lloyd (1990) reports on two years of rainfall data from a *terra firme* forest near Manaus. The term *terra firme* refers to the dense, humid, evergreen forests of the Amazon basin that do not flood annually. Although three hours was generally sufficient for throughfall drip and stemflow to stop and for the upper and mid-levels of the canopy to dry, the humid climate meant that it took longer for the foliage and bark closer to the forest floor to dry. Less than 13% of days with rainfall had more than one storm, with the majority of storms occurring during the day. There was no trend between storm duration and rainfall rate observed. This data suggests that for models on daily or longer time scales, it may be reasonable to assume that intercepted water evaporates from the canopy before the arrival of the next storm and that the amount of water intercepted in the subsequent storm is not significantly reduced due to an already saturated canopy.

Ubarana (1996) reports on measurements of rainfall partitioning in two *terra firme* forests, one near Ji-Paraná, Rondônia and the other located near Marabá in Pará state (Figure 2.1). Hourly rainfall was measured with a tipping bucket; throughfall and stemflow were measured weekly. Collections were made for several individual rain events, allowing throughfall to be linearly regressed against gross rainfall. The canopy storage capacities estimated from these relationships were 1.03 mm (Rondônia) and 1.25 mm (Pará). This is similar to the 1.12 mm storage used by Ashby (1999) for a forest in Rondônia. Trunk storage capacity was only 0.09-0.10 mm. Average total throughfall was 86.2-87% of gross rainfall, with interception taking up 11.6-12.9%. Stemflow was less than 1.5% in both forests. Interception varied considerably between collections. The

data also demonstrated that most interception occurred at rainfall intensities <10 mm $hr^{-1}$, and became almost insignificant at higher rates. When the intensity was 1-2 mm $hr^{-1}$, interception could be as high 60-70% of the incoming rainfall.

**Evapotranspiration**

Evaporation and transpiration are the mechanisms by which water is returned to the atmosphere. The driving force for this transfer of water vapor is a gradient in vapor pressure between the air and the evaporating surface (Kramer and Boyer 1995). The gradient will be governed by factors such as air temperature, net solar radiation, air humidity, and wind (Dunne and Leopold 1978). The components of evapotranspiration in forests include evaporation from the soil surface and wet leaves, and transpiration by vegetation. Water stored on the leaves generally evaporates more readily than it transpires through leaf stoma (Ubarana 1996), while soil surface evaporation is a negligible component of the water budget in closed canopy forests of the Amazon, usually on the order of 1-5 mm per month (Leopoldo et al. 1995; Delire et al. 1997).

Potential evapotranspiration (PET) is the highest possible rate of vapor transfer and is determined primarily by atmospheric conditions. The actual rate of evapotranspiration (AET) may be less than PET when water is deficient (Dunne and Leopold 1978). Transpiration losses may exceed rainfall inputs on a given day or for many months during the dry season (Hodnett et al. 1996; Jipp et al. 1998). Despite this potential for excess transpiration, during relatively normal rainfall years, AET and PET rates are similar for intact forests in the central Amazon during most of the year (Leopoldo et al. 1995). This is probably not true when drought conditions persist.

As long as an adequate supply of water is stored in the soil, transpiration may be higher in the dry season compared to the wet season (Delire et al. 1997). This higher transpiration rate is due to the greater vapor pressure deficit between leaves and the atmosphere. However, as water is extracted and the soil dries out, resistance to uptake in the roots will increase and transpiration may again be limited (Jipp et al. 1998).

In general, more than half of the precipitation coming into the Amazon River basin will be evapotranspired (Nobre et al. 1991). Leopoldo et al. (1995) constructed a three-year water balance for the Barro-Branco watershed in central Amazonia north of the city of Manaus. They determined that the average ET was 1493 mm, representing more than 67% of rainfall. Transpiration was 1243 mm of the total ET. Ribeiro and Villa Nova (1979) estimated an annual PET for a *terra firme* forest of 1536 mm $year^{-1}$ (4.2 mm $day^{-1}$) while Villa Nova et al. (1976) estimated that the PET of the entire Amazon basin is 1460 mm $year^{-1}$ (4.0 mm $day^{-1}$). The actual annual ET totals reported by these studies were 1508 mm and 1168 mm, respectively (both articles are cited in Leopoldo et al., 1995). Both AET values are on the order of Jipp et al. (1998), who used a soil water balance to calculate an annual ET of 1514 mm (4.15 mm $day^{-1}$) for an eastern forest in Paragominas. A somewhat lower total of 1350 mm (3.7 mm $day^{-1}$) was determined for another eastern forest located just east of Belém using a matric-potential reduction function (Klinge et al. 2001).

Many methods exist for calculating potential evapotranspiration from meteorological data. One of the earlier methods was developed by Thornthwaite (Thornthwaite 1948; Thornthwaite and Mather 1957). Assuming that air temperature

largely incorporates the effects of other meteorological variables, the Thornthwaite formula for potential evapotranspiration (PET, cm month$^{-1}$) is:

$$PET = 1.6C\left(\frac{10T_i}{I}\right)^a \qquad [2.1]$$

where $T_i$ is the monthly air temperature (ºC) for month i, C is a coefficient accounting for daylight and I is the annual heat index equal to:

$$I = \sum_{i=1}^{12}\left[\frac{T_i}{5}\right]^{1.51} \qquad [2.2]$$

and a is an exponent derived from the annual heat index:

$$a = 0.49 + 0.0179\,I - 0.0000771\,I^2 + 0.000000675\,I^3 \qquad [2.3]$$

The monthly PET estimate may be adjusted for the number of daylight hours in a month based on the site latitude. Other correction factors have been developed for sites outside of the temperate climate for which the Thornthwaite method was empirically established (Amorim et al.1999).

**Mathematical models to describe water flow in soil**

It is clear from the studies of rainfall partitioning and evapotranspiration that large quantities of water are cycled within the Amazon River basin. When this cycle is disrupted and precipitation declines, how will infiltration and redistribution of water in the soil be affected? While various methods have been used to make estimates of soil moisture at a given point in time, mathematical models are used to describe the magnitudes and rates of water fluxes.

Water moves in soil due to a difference in potential energy, usually expressed as a pressure or head. Water moves from high to low potential until equilibrium is reached

(Hillel 1980). Darcy's Law states that the drop in this potential per unit distance, which is known as the hydraulic gradient, is proportional to the water flux. The proportionality factor relating water flux to the hydraulic gradient is called the hydraulic conductivity (Soil Science Society of America 1997). In saturated soils, potential differences are mostly due to the sum of elevation and pressure heads, and hydraulic conductivity is largely independent of these forces. In unsaturated soils, differences in potential are also influenced by capillarity and adsorption resulting from the affinity of water molecules to the pores and particles of the soil. The term matric potential is usually used to describe these forces. The hydraulic conductivity varies with the magnitude of the matric potential. Therefore, in unsaturated soils, hydraulic conductivity must be determined as a function of matric potential or water content. Buckingham (1907) modified Darcy's law for saturated water flow to apply to unsaturated conditions:

$$q = -K(h)\frac{\partial H}{\partial z} \qquad [2.4]$$

where q is the is the steady water flux (cm $day^{-1}$), K(h) is the unsaturated hydraulic conductivity (cm $day^{-1}$), H is the total head potential (cm), and z is the flow distance in the vertical direction (cm).

Mathematical models have been promoted as a less expensive and faster way to estimate unsaturated hydraulic conductivity because of the difficulties associated with laboratory and field methods. It is easier to scale results across a landscape once a model has been proven to successfully predict for a range of soils (Mualem 1976).

Mualem (1976) proposed a mathematical model to predict unsaturated hydraulic conductivity from saturated conductivity and soil water retention data. The model considers the soil to be a collection of capillary tubes, with factors considering the

tortuosity between the tubes and the degree of saturation of the soil. In a comparitive study, the Mualem model out-performed existing equations in predicting unsaturated hydraulic conductivity for 45 soils for which data on the conductivity-water content and water content-matric potential relationships were available (Mualem 1976). An equation for better describing the soil water content-matric potential curve was subsequently developed (van Genuchten 1980):

$$\theta(h) = \theta_r + \left[\frac{\theta_s - \theta_r}{1 + (\alpha h)^n}\right]^{1-\frac{1}{n}} \qquad [2.5]$$

where θ(h) is the volumetric water content ($cm^3\ cm^{-3}$) at a given potential h, $\theta_s$ and $\theta_r$ are the saturated and residual water contents, respectively, α is a fitting parameter describing the shape of the curve ($cm^{-1}$), and n is a dimensionless fitting parameter affecting the steepness of the curve. The $\theta_r$ parameter defines where the slope of the water characteristic curve levels out, in theory representing the condition where water is strongly absorbed to particle surfaces and fluid will not flow. Since $\theta_s$, is the water content at saturation, it is a reflection of the total porosity of a soil. Soils with larger pores that release a lot of water with small changes in h have high values of α, and vice versa (Hodnett and Tomasella 2002). When the van Genuchten (1980) water retention equation is combined with the Mualem (1976) model for unsaturated hydraulic conductivity K(θ), the new model is:

$$K(\theta) = K_s\left(\frac{\theta - \theta_r}{\theta_s - \theta_r}\right)^{1/2}\left[1 - \left(1 - \left(\frac{\theta - \theta_r}{\theta_s - \theta_r}\right)^{\left(n/(n-1)\right)}\right)^{(n-1)/n}\right]^2 \qquad [2.6]$$

Although they work well for many soil types, the Mualem and van Genuchten equations only apply to soils with flow through capillary pores. If the soil has developed a structure involving continuous macropores, water may infiltrate faster and deeper than predicted by the equations by bypassing most of the total cross-sectional area of soil.

Michiels et al. (1989) compared field, laboratory and mathematical models for predicting unsaturated hydraulic conductivity in the study of a coarse-textured soil. The field method chosen was the instantaneous profile method. Mualem's mathematical model was also tested, using van Genuchtens's equation to characterize the soil water content-matric potential relationship. The results showed that van Genuchten's equation best described soil water data that had been derived by a pressure plate method. Van Genuchtens's equation was easier to use for medium and fine-textured soils that do not have well-defined air entry values required by other models. Overall, the authors concluded that mathematical models are a good way to predict unsaturated hydraulic conductivity.

**Modeling Plant Uptake**

Drought may impact plant uptake patterns by altering atmospheric conditions that determine the vapor pressure gradient between air and leaves and by lowering the amount of water in the soil available to be extracted. Roots serve as an important link between the above and below-ground components of water and nutrient cycles. Soil water content and hydrology, as well as root abundance and functionality all affect the partitioning and total amount of water taken up from soil.

The approaches to modeling root water uptake have been separated into two general classes: microscopic and macroscopic. The main difference is that microscopic models consider the geometry and distribution of individual roots and the properties of roots, plants, and soil that influence water extraction whereas macroscopic models consider the root system to be a single, diffuse sink in each layer of the root zone (Mathur and Rao 1999; Feddes et al. 2001). Mathematically this sink can be represented by a term added to the equation for unsaturated water flow:

$$q = \left( - K(h) \frac{\partial H}{\partial z} \right) - U(z) \qquad [2.7]$$

Atmospheric demand for water vapor is what drives the amount and rate of soil water uptake in macroscopic models. Uptake in a given layer is proportional to the potential evapotranspiration rate and root abundance in that layer:

$$U(z) = PET \cdot root(z) \cdot RF \qquad [2.8]$$

where U(z) is plant uptake (cm $day^{-1}$) at a given depth, PET is the potential evapotranspiration (cm $day^{-1}$), root(z) is the fraction of total root length density in a given layer z, and RF is a function reducing uptake from that layer based on some estimate of water stress. When soil moisture is optimal, the total extraction from the root zone is equal to potential evapotranspiration (PET). When soil moisture is either limiting or excessive, root water uptake is reduced from this maximum rate by the RF function reflecting the moisture condition of the soil. In wet soils, water has high potential energy and so is freer to move around and be taken up by plants. In dry soils, water is bound more tightly to soil particles, giving it a lower potential energy and making it harder for plants to remove it. With increased drying, the soil water eventually reaches such a low potential energy that it cannot be transported to plant roots quickly enough to prevent

wilting. The water content at this matric potential is called the permanent wilting point ($\theta_{WP;}$ Kramer and Boyer 1995).

The Food and Agricultural Organization of the United Nations (FAO) has developed a methodology to estimate actual evapotranspiration under conditions of water stress (Figure 2.2). Noting that meteorological factors such as vapor pressure deficit, solar radiation, and wind, as well as vegetation characteristics, soil water content and the ability of soil to conduct water to roots all influence transpiration rates, the FAO method uses the water stress coefficient, $K_s$, to reflect the decrease in water uptake as soils dry. The FAO water stress coefficient is based on the ratio of "readily available water" (RAW) to "total available water" (TAW) in the root zone. Water that is retained in a soil after internal drainage has ceased is considered to be at field capacity ($\theta_{FC}$). The total available water is the total amount of water between field capacity and wilting point ($\theta_{FC}$-$\theta_{WP}$). The theory behind RAW is that plant uptake is reduced before wilting point is reached, so RAW is the amount that plants can easily take up before they experience severe water stress. The proportion of TAW that is readily available will vary for different species of plants, and also varies with the evaporative demand of the atmosphere. Once the water content drops past a threshold value, meaning all of the RAW has been extracted, $K_s$ is used to reduce evapotranspiration rates in proportion to the amount of water remaining. Above that threshold, $K_s$ is at unity and evapotranspiration occurs at the maximum rate (Allen et al. 1998).

Similar reduction functions based on potential energy of soil water (pressure head) have been used (Feddes et al. 1978; Prasad 1988). These functions assume that the potential of the soil water at a given depth will determine how much water roots can

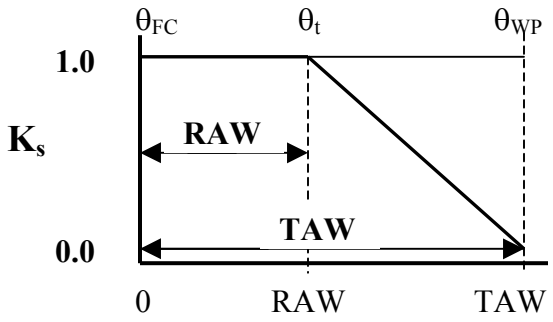


**Figure 2.2 Plant uptake reduction function based on available water. The water stress coefficient, $K_s$, is used to reduce evapotranspiration from the maximum rate ($K_s$=1) after all readily available water (RAW) has been extracted. Total available water (TAW) is defined as the water held between field capacity ($\theta_{FC}$) and wilting point ($\theta_{WP}$).**

extract from that layer (Figure 2.3). At water pressures above h1, the soil is too wet for sufficient aeration and uptake is inhibited due to the oxygen deficiency. Above h2, root uptake is limited and quickly reaches zero. Between h2 and h3, non-limiting moisture conditions allow for water uptake at the maximum rate, which is equal to PET. The water pressure at h4 represents wilting point; if the soil is drier than wilting point uptake is zero. When evaporative demand is high, uptake rates are slower at higher soil water pressure heads (Yang and de Jong 1972). Some reduction functions allow h3 to vary with the potential transpiration rate (Mathur and Rao 1999). The function follows h3h when PET is higher and follows h3l when evaporative demand is lower.

In addition to relations of root uptake and water potential, other investigators have looked at root uptake with soil depth or root age. The ratios of naturally abundant stable isotopes have allowed indirect inference of root water uptake patterns with depth (Moreira et al. 2000). Dawson (1998) used relative water contents to indicate water availability and proportion root water uptake at a given depth of soil relative to other depths. However, other researchers have noted that the presence of roots at a given depth does not mean that those roots are being fully utilized (Ehleringer and Dawson 1992; Moreira et al. 2000). Soil temperature and root age can affect root functionality. Thorburn and Ehleringer (1995) confirmed that roots do tend to extract water from the most available source, but that the relationship between water availability and uptake is not always straightforward. In their study, they found examples of roots that did not take up significant amounts of water despite being located in soil where water was apparently available. Based on stable isotope ratios in root water compared to soil, they also found evidence that water recovered from roots had not been taken up entirely from

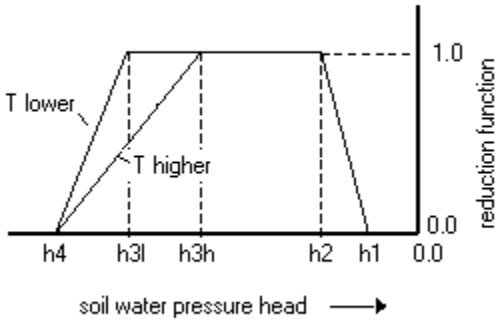


**Figure 2.3 Plant uptake reduction function based on pressure head. Between pressure heads h2 and h3, soil moisture is non-limiting and plant uptake is not restricted. The function may follow T higher when potential evapotranspiration is high and T lower when it is low. At pressure heads greater than h1 or lower than the wilting point at h4, plant uptake is zero.**

surrounding soil. Partitioning uptake for different depths in proportion to root presence assumes that roots function equally well at taking up available water around them. Depending on the degree to which this assumption is violated, functions that partition uptake based on roots may not be able to capture uptake patterns accurately.

**Rooting Depth and the Role of Deep Soil Water in the Amazon**

By storing water that vegetation can extract later, soil moderates the impact of fluctuations in water inputs and buffers vegetation against physiological stress. Comparisons of evapotranspiration measurements with water balance estimates of soil water storage from an Amazonian forest have indicated that transpiration decreases very little during normal dry periods (Hodnett et al. 1996; Delire et al. 1997). Of course the effectiveness of the soil reservoir in buffering plants from stress depends on the size and availability of the water reserves it holds. The lateral extent and depth to which a rooting system reaches defines the total volume from which it can extract water. Some studies have shown that deep roots (>one meter) are common under the closed canopy forests of the Amazon (e.g. Nepstad et al. 1994; Carvalheiro and Nepstad 1996), but there has been some uncertainty over the exact role of deep roots in forest hydrology since they have also been found in areas that do not seem to require them at least annually (Nepstad et al. 1994).

More than one-third of the Amazon region is inhabited by evergreen forests that receive less than 1.5 mm of rain per day during the driest months of the year (Nepstad et al. 1994). These forests are thought to maintain their evergreen canopies by relying on

soil water extracted from deeper layers of the soil during the time when potential evapotranspiration exceeds new rainfall inputs.

Nepstad et al. (1994) completed a study of deep rooting in pastures and forests near the town of Paragominas, Pará, in eastern Amazonia. Not surprisingly, fine-root biomass was more abundant near the soil surface. While levels of fine-root biomass under the forest remained relatively steady below 50 centimeters, some roots extended to depths as great as 18 meters. Comparing satellite imagery with estimates of canopy greenness, the authors estimated that about half of the Amazon's forests rely on deep rooting to access stored soil water during the annual dry season. Plant available water (PAW) was monitored using a soil water balance approach during a severe dry season in 1992. It was estimated that more than 75% of the water extracted from the soil was from the PAW portion below two-meters in the soil.

Another study of the hydrologic effects of landuse change near Paragominas supports the conclusion that primary forest can extract water from soil layers deeper than two meters (Jipp et al. 1998). Hydrologic budgets were made for adjacent tracts of mature primary forest, re-growing secondary forest, and pasture over four years. Plant available water (PAW) between two and eight meters was depleted during the first dry season, and was not completely recharged until after a two-year El Niño event had passed. Recharge of soils at depth lagged behind that of the top profile of soil, suggesting that the water was infiltrating as a wetting front. Drainage to the water table was limited until deep soil layers were completely recharged.

Moreira et al. (2000) used stable isotopes to examine vertical patterns of plant uptake from deep soil in forest and pasture. Working at the same Paragominas study site

as Nepstad et al. (1994) and Jipp et al. (1998), they irrigated 2 x 2 meter plots with deuterium and then analyzed soil water and stem water of small trees. The authors theorized that diverse plant species are able to coexist in these tropical forests by exploiting different volumes of the soil. Although this hypothesis was not substantiated, the study was able to confirm that forest trees extracted substantial amounts of water from below the top meter of soil.

Another irrigation experiment using deuterium-labeled water was conducted in a central Amazonian forest south of the city of Santarém (Sternberg et al. 2002). Over the course of the study, the highest water uptake occurred between the soil surface and two meters depth, with a majority of that coming from the top 0.5 meters. This is much shallower uptake than was observed at the Paragominas site (Moreira et al. 2000). Several possible reasons for this difference were discussed, including the unusually rainy dry season that preceded the study period and the possibility that labeled water at depth was diluted by water uptake from shallower soil. Since only small trees were sampled, it may be that vertical patterns of uptake are different than with larger and more mature trees. Finally, soil water uptake at depth may occur primarily when the surface soil dries out and trees allocate more resources to root production at depth in order to tap those water reserves. Uptake patterns also suggested that that a central core of roots was associated with the main stem of each individual tree, but that there were some lateral roots extending as far away as 10 meters from the core.

Hodnett et al. (1995) completed a water balance for a central Amazonian forest north of Manaus, Amazonas. Data from neutron probes installed to two meters depth revealed that all of the plant-available water in the upper two meters was exploited during

the two dry seasons analyzed. Theoretically, vegetation would experience less resistance to taking up available water from wetter horizons below than to extract water from drier horizons with strongly negative potentials and correspondingly lower hydraulic conductivities. They concluded that during drier than normal years, the forest must extract water from below two meters. In a later water balance analysis of the same area, a long-term record of soil moisture revealed that root water uptake from below two meters did occur in all 27 years of the record (Hodnett et al. 1996). The calculated evaporative demand could not be maintained by the observed changes in water content in the top two meters and it was estimated that the required water would need to come from as far down as 9 meters. Water was extracted from all layers simultaneously and was not sequential.

These studies of rooting depth and deep soil water uptake in humid tropical forests provide important guidance for modeling. They show that the forests root deeply and that uptake of water from deeper soil layers is important, especially during dry periods. Many models of forest water cycling have assumed that all plant uptake comes from the upper two meters of soil. The conclusion that water is taken up from all layers simultaneously would suggest that the "tipping bucket" approach, whereby plant uptake is satisfied by emptying soil layers sequentially, is not well-suited to these forests.

**Water Movement and Storage Properties of Amazon Oxisols**

Latosols of Brazilian taxonomy correspond to Oxisols of the U.S. soil taxonomy (Bernoux et al. 1998). Typical Brazilian Oxisols are characterized by high clay contents, low silt contents, and high porosity (low bulk density) with many stable microaggregates.

The generally greater depths and different mineralogy, structure and texture of Amazon Oxisols reflect the many thousands of years that they have been weathering in the absence of glacial activity. The soils are typified by low fertility and accumulation of Fe and Al (Hodnett and Tomasella 2002). Amazon soils under mature forest can be relatively heterogeneous due to the action of soil fauna such as ants, termites, and worms (Carvalheiro and Nepstad 1996). In general, surface infiltration in clayey Oxisols of the Amazon is faster than clay soils of temperate regions (Delire et al. 1997). Hodnett et al. (1995) noted the absence of surface runoff on undisturbed forest soils under a central Amazonian forest, even during the most intense rains.

The bimodal nature of the porosity between macro and micropores in Amazon Oxisols has been discussed in several studies (e.g. Chauvel et al., 1991). As mentioned above, a significant fraction of the total porosity comes from macropores, but an even greater proportion consists of micropores within the stable aggregates. The presence of many stable aggregates in tropical Oxisols means that water can infiltrate and move fast at low tensions (like a sand) and is held tightly at high tensions (like a clay; Tomasella and Hodnett 1998). Once the exterior of the aggregates is saturated, water is able to flow rapidly though the larger pores between them, while water inside of the aggregates remains relatively immobile (Sollins and Radulovich 1988).

Carvelheiro and Nepstad (1996) documented the presence of chambers and soft spots in an Oxisol under forest in Paragominas, Pará in the eastern Amazon. Such large voids could allow water to percolate while bypassing much of the soil volume. The hydraulic conductivity for this type of flow would not be predicted well by the Mualem model because the model assumes that water moves down through the soil matrix

(Mualem 1976). Moreira et al. (2000) irrigated plots with deuterium in an abandoned pasture and primary forest in the same area as the Carvalheiro and Nepstad (1996) study. Soil cores from various depths and stem samples from two liana species and four tree species were collected from the forest plots. The water in these plant and soil samples was then extracted and analyzed for the presence of the deuterium label. Movement of the deuterium pulse suggested that water moves as piston flow, with new rainfall inputs displacing water already in the soil and pushing it down deeper instead of mixing with it. This result implies that preferential flow, whereby water moves through macropores and bypasses most of the soil matrix, was not important in those soils.

Researchers working near Ji-Paraná in Rondônia measured saturated hydraulic conductivity ($K_{sat}$) from 5-15 centimeters depth with a Guelph permeameter and down to 1 meter with an amoozemeter (Elsenbeer et al. 1999). The hydraulic conductivities of this top meter were lower than values reported for the central Amazon. The authors caution that while many soils in the Amazon basin have been shown to have high permeability, variability in this property could make the common assumption of predominantly vertical water flow untrue. There is enough heterogeneity within the Amazon and even within the same soil orders (such as latosols) that the $K_{sat}$ of a particular site needs to be measured before local patterns of water flow can be determined with any meaningful accuracy.

Sternberg et al. (2002) reported the results of a study of plant water uptake under a *terra firme* forest of the central Amazon, south of the city of Santarém, Pará (Figure 2.1). Two 2x2 meter forest plots were irrigated with a pulse of deuterium, and then soil water and plant samples were analyzed for presence of the label at four later dates. The

estimated percolation rate of the pulse was 0.25 m month$^{-1}$. Label migration in the soil occurred during the heaviest rains but there was very little lateral movement. Moreira et al. (2000) measured a percolation rate of deuterated water at 0.15 m month$^{-1}$ in Paragominas, Pará, and also found lateral flow to be minimal. Differences in the pulse percolation rates may be due to differences in rainfall distribution and initial soil moisture between the two sites. Drainage in these Oxisols under *terra firme* forest is frequently rapid, which tends to dampen the effect of spikes in water input on water storage (Hodnett et al. 1995). Although new water inputs require several months to reach deeper horizons, responses to changes in water contents at the surface can be detected much sooner (Jipp et al. 1998).

Most available water in clayey Brazilian Oxisols is held at tensions below –100 kPa (Tomasella and Hodnett 1998). Many studies have confirmed that these clay-rich deeply-rooted Oxisols have low plant-available water (Nepstad et al. 1994; Hodnett et al. 1996; Jipp et al. 1998). Tomasella and Hodnett (1996) estimated available water capacity of an Oxisol under pasture to be only 70 mm month$^{-1}$ in the upper meter of soil. Jipp et al. (1998) reported plant-available water (PAW) for the upper eight meters of soil under mature forest to range from 56 mm after the 1992 dry season to 941 mm after the 1994 wet season. Low PAW relates to the high clay texture and micro-aggregated structure of the soil. Soils with more sand and silt particles tend to hold water less tightly and therefore have higher proportions of PAW.

Tomasella et al. (2000) performed multiple linear regressions between data on water retention and other properties for Brazilian soils. The van Genuchten residual water content ($\theta_r$), conceptually defined as the point when only water adsorbed to particle

surfaces remains in the soil, was assumed to correspond to the water content at –1500 kPa. The water content at –1500 kPa tension is commonly used to represent the wilting point for vegetation. However, the very fine pores of these soils only empty at tensions greater than –4000 kPa (Chauvel et al. 1991). The residual water contents ($\theta_r$) fit from the Tomasella et al. (2000) survey of lab-generated water retention data were found to be quite high, averaging 0.187 $m^3m^{-3}$. This is not unexpected given the high clay contents, but a field study by Jipp et al. (1998) frequently measured dry season soil moisture under mature forest lower than the water contents corresponding to –1500 kPa tension.

A higher percentage of tropical soils fit into clay textural classes than do temperate soils (Hodnett and Tomasella 2002). Van Genuchten parameters derived from water retention information for 771 horizons included in a database of tropical soils had, on average, high $\alpha$, $\theta_r$, and $\theta_s$. The average $\theta_r$ was 0.27 $m^3m^{-3}$ for tropical soils, compared to 0.11 $m^3m^{-3}$ for temperate soils. The high $\alpha$ value implies better structure and more macroporosity, which leads to large changes in water content with small changes in pressure as pores empty. High $\theta_s$ values demonstrate high total porosity. The very high residual water contents reflect the high specific surface of the soil particles, whereas rapid changes between saturation and field capacity is indicative of macropores (Sollins and Radulovich 1988).

Buttler and Riha (1992) compared two approaches to modeling soil water flow using data from cerrado Oxisols near Brasília, Distrito Federal. Input data included saturated hydraulic conductivity, which was highly negatively correlated with bulk density. One model involved capacity water flow (commonly referred to as a "tipping bucket" approach) combined with an uptake term based on plant available water. The

other model used the Richards' equation for transient unsaturated water flow with plant uptake determined by soil water potential. The tipping bucket approach predicted average water contents well, but was not able to capture the changes in water content with depth over time as well as the Richards' model.

The studies of Amazon hydrology and soil properties that have been reviewed here provide useful information for modeling soil water dynamics. Specifically, they may be used to evaluate whether simplifying assumptions inherent in a model's structure, the model input, and the resultant output are reasonable. Climate studies have demonstrated that the intensity and duration of seasonal droughts have increased in recent decades, and models have predicted continued reductions in rainfall due to global climate change and/or land use conversion. It is important to understand how tropical moist forests will tolerate such prolonged drought, given their global importance in the exchange of water, elements, and energy.

## References

Allen, R. G., L. S. Pereira, D. Raes and M. Smith (1998). Crop evapotranspiration- Guidelines for computing crop water requirements. Rome, FAO- Food and Agriculture Organization of the United Nations**:** Irrigation and Drainage Paper 56.

Amorim, M. C. d., L. Rossato and J. Tomasella (1999). Determinação da evapotranspiração potential do Brasil aplicado o modelo de Thornthwaite a um sistema de informação geografica. Revista Brasileira de Recursos Hidricos 4(3): 83-90.

Ashby, M. (1999). Modelling the water and energy balances of Amazonian rainforest and pasture using Anglo-Brazilian Amazonian climate observation study data. Agricultural and Forest Meteorology 94: 79-101.

Bernoux, M., D. Arrouays, C. Cerri, B. Volkoff and C. Jolivet (1998). Bulk densities of Brazilian Amazon soils related to other soil properties. Soil Science Society of America Journal 62: 743-749.

Broecker, W. S. (1996). The once and future climate. Natural History 105(9): 30-40.

Bruijnzeel, L. A. (1996). Predicting the hydrological impacts of land cover transformation in the humid tropics: the need for integrated research. *In* Amazonian Deforestation and Climate. J. H. C. Gash, C. A. Nobre, J. M. Roberts and R. L. Victoria. John Wiley and Sons, New York**:** 15-55.

Buckingham, E. (1907). Studies on the movement of soil moisture, USDA Bulletin 38.

Buttler, I. W. and S. J. Riha (1992). Water fluxes in oxisols: a comparison of approaches. Water Resources Research 28(1): 221-229.

Carvalheiro, K. d. O. and D. C. Nepstad (1996). Deep soil heterogeneity and fine root distribution in forests and pastures of eastern Amazonia. Plant and Soil 182: 279-285.

Chauvel, A., M. Grimaldi and D. Tessier (1991). Changes in soil pore-space distribution following deforestation and revegetation: an example from the central Amazon basin, Brazil. Forest Ecology and Management 38: 259-271.

Cochrane, M. and M. D. Schulze (1998). Forest fires in the Brazilian Amazon. Conservation Biology 12(5): 948-950.

Costa, M. H. and J. A. Foley (2000). Combined effects of deforestation and doubled atmospheric CO2 concentrations on the climate of Amazonia. Journal of Climate 13: 18-34.

Dai, A., K. E. Trenberth and T. R. Karl (1998). Global variations in droughts and wet spells: 1900-1995. Geophysical Research Letters 25(17): 3367-3370.

Dawson, A. G. and G. O'Hare (2000). Ocean-atmosphere circulation and global climate: The El-Nino-Southern Oscillation. Geography 85: 193-208.

Dawson, T. E. (1998). Fog in the California redwood forest: ecosystem inputs and use by plants. Oecologia 117: 476-485.

Delire, C., J. C. Calvet, J. Noilham, I. Wright, A. Manzi and C. A. Nobre (1997). Physical properties of Amazonian soils: a modeling study using the Anglo-Brazilian Climate Observation Study data. Journal of Geophysical Research 102(D25): 30119-30133.

Dunne, T. and L. B. Leopold (1978). Water in Environmental Planning. W.H. Freeman and Company, New York. 818p.

Ehleringer, J. R. and T. E. Dawson (1992). Water uptake by plants: perspective from stable isotope composition. Plant, Cell and Environment 15: 1073-1082.

Elsenbeer, H., B. E. Newton, T. Dunne and J. M. de Moraes (1999). Soil hydraulic conductivities of latosols under pasture, forest, and teak in Rhondonia, Brazil. Hydrological Processes 13: 1417-1422.

Entekhabi, D., I. Rodriguez-Iturbe and F. Castelli (1996). Mutual interaction of soil moisture state and atmospheric processes. Journal of Hydrology 184: 3-17.

Feddes, R. A., H. Hoff, M. Bruen, T. E. Dawson, P. de Rosnay, P. Dirmeyer, R. B. Jackson, P. Kabat, A. Kleidon, A. Lilly and A. J. Pitman (2001). Modeling root water uptake in hydrological and climate models. Bulletin of the American Meteorological Society 82(12): 2797-2809.

Feddes, R. A., P. J. Kowalik and H. Zaradny (1978). Simulation of Field Water Use and Crop Yield. Centre for Agricultural Publishing and Documentation, Wageningen. 189p.

Gash, J. H. C., C. A. Nobre, J. M. Roberts and R. L. Victoria (1996). An overview of ABRACOS. *In* Amazonian Deforestation and Climate. J. H. C. Gash, C. A. Nobre, J. M. Roberts and R. L. Victoria. John Wiley and Sons, New York: 1-14.

Hillel, D. (1980). Fundamentals of Soil Physics. Academic Press, San Diego. 413p.

Hodnett, M.G., M. D. Oyama, J. Tomasella and A. de O Marques Filho (1996). Comparisons of long-term soil water storage behaviour under pasture and forest in three areas of Amazonia. *In* Amazonian Deforestation and Climate. J. H. C. Gash, C. A. Nobre, J. M. Roberts and R. L. Victoria. John Wiley and Sons, New York**:** 57-77.

Hodnett, M.G., L. Pimental da Silva, H. R. da Rocha and R. Cruz Senna (1995). Seasonal soil-water storage changes beneath central Amazonian rainforest and pasture. Journal of Hydrology 170: 233-254.

Hodnett, M.G. and J. Tomasella (2002). Marked differences between van Genuchten soil water-retention parameters for temperate and tropical soils: new water-retention pedo-transfer functions developed for tropical soils. Geoderma 108: 155-180.

Hodnett, M.G., J. Tomasella, A. de O Marques Filho and M. D. Oyama (1996). Deep soil water uptake by forest and pasture in central Amazonia: predictions from long-term daily rainfall data using a simple water balance model. *In* Amazonian Deforestation and Climate. J. H. C. Gash, C. A. Nobre, J. M. Roberts and R. L. Victoria. John Wiley and Sons, New York**:** 79-99.

Jipp, P. H., D. C. Nepstad, K. Cassel and C. R. de Carvalho (1998). Deep soil moisture storage and transpiration in forests and pastures of seasonally-dry Amazonia. Climate Change 39: 395-413.

Kaufman, Y. J. and R. S. Fraser (1997). The effect of smoke particles on clouds and climate forcing. Science 277(5332): 1636-1639.

Klinge, R., J. Schmidt and H. Folster (2001). Simulation of water drainage of a rain forest and forest conversion plots using a soil water model. Journal of Hydrology 246: 82-95.

Kousky, V. E., M. T. Kagano and I. F. A. Cavalcanti (1984). A review of the Southern Oscillation: oceanic-atmospheric circulation changes and related rainfall anomolies. Tellus 36A: 490-504.

Kramer, P. J. and J. S. Boyer (1995). Water Relations of Plants and Soils. Academic Press, San Diego. 495p.

Lean, J., C. B. Bunton, C. A. Nobre and P. R. Rowntree (1996). The simulated impact of Amazonian deforestation on climate using measured ABRACOS vegetation characteristics. *In* Amazonian Deforestation and Climate. J. H. C. Gash, C. A. Nobre, J. M. Roberts and R. L. Victoria. John Wiley and Sons, New York**:** 549-576.

Leopoldo, P. R., W. K. Franken and N. Augusto Villa Nova (1995). Real evapotranspiration and transpiration through a tropical rain forest in central Amazonia as estimated by the water balance method. Forest Ecology and Management 73: 185-195.

Llyod, C. R. (1990). The temporal distribution of Amazonian rainfall and its implications for forest interception. Quarterly Journal of the Royal Meteorogical Society 116: 1487-1494.

Marin, C. T., W. Bouten and J. Sevink (2000). Gross rainfall and its partitioning into throughfall, stemflow and evaporation of intercepted water in four forest ecosystems in western Amazonia. Journal of Hydrology 237: 40-57.

Mathur, S. and S. Rao (1999). Modeling water uptake by plant roots. Journal of Irrigation and Drainage Engineering 125(3): 159-165.

Michiels, P., R. Hartmann and E. De Strooper (1989). Comparisons of the unsaturated hydraulic conductivity of a coarse-textured soil as determined in the field, in the laboratory, and with mathematical models. Soil Science 147(4): 299-304.

Moreira, M., L. d. S. L. Sternberg and D. C. Nepstad (2000). Vertical patterns of soil water uptake by plants in a primary forest and abandoned pasture in the eastern Amazon: an isotopic approach. Plant and Soil 222: 95-107.

Moreira, M. Z., L. D. L. Sternberg, L. A. Martinelli, R. L. Victoria, E. M. Barbosa, L. C. M. Bonates and D. C. Nepstad (1997). Contribution of transpiration to forest ambient vapour based on isotopic measurements. Global Change Biology 3: 439-450.

Morengo, J., B. Liebmann, V. E. Kousky, N. Filizola and I. Wainer (2001). On the onset and the end of the rainy season in the Brazilian Amazon Basin. Journal of Climate 14: 833-852.

Mualem, Y. (1976). A new model for predicting the hydraulic conductivity of unsaturated porous media. Water Resources Research 12(3): 513-522.

Nepstad, D. C., P. Moutinho, M. B. Dias-Filho, E. Davidson, G. Cardinot, D. Markewitz, R. Figueiredo, N. Vianna, J. Chambers, D. Ray, J. B. Guerreiros, P. Lefebvre, L. Sternberg, M. Moreira, L. Barros, F. Y. Ishida, I. Tohlver, E. Belk, K. Kalif and K. Schwalbe (2002). The effects of partial throughfall exclusion on canopy processes, aboveground production, and biogeochemistry of an Amazon forest. Journal of Geophysical Research 107(D20): 8085, doi: 10.1029/2001JD000360.

Nepstad, D. C., C. R. de Carvalho, E. A. Davidson, P. H. Jipp, P. A. Lefebvre, G. H. Negreiros, E. D. da Silva, T. A. Stone, S. E. Trumbore and S. Viera (1994). The role of deep roots in the hydrological and carbon cycles of Amazonian forests and pastures. Nature 372: 666-669.

Nepstad, D. C., C. Uhl, C. A. Pereira and J. M. C. da Silva (1996). A comparative study of tree establishment in abandoned pasture and mature forest of eastern Amazon. Oikos 76: 25-39.

Nobre, C. A., P. J. Sellers and J. Shukla (1991). Amazonian deforestation and regional climate change. Journal of Climate 4: 957-988.

Prasad, R. (1988). A linear root water uptake model. Journal of Hydrology 99: 297-306.

Ribeiro, M. d. N. G. and N. A. Villa Nova (1979). Estudo climatológico da Reserva Florestal Ducke. III. evapotranspiração. Acta Amazonica 9: 305-309.

Rogers, J. C. (1988). Precipitation variability over the Caribbean and tropical Americas associated with the Southern Oscillation. Journal of Climate 1: 172-182.

Ropelewski, C. F. and M. S. Halpert (1987). Global and regional scale precipitation patterns associated with the El Nino/Southern Oscillation. Monthly Weather Review 115: 1606-1626.

Rosenfeld, D. (1999). TRMM observed first direct evidence of smoke from forest fires inhibiting rainfall. Geophysical Research Letters 26: 3105-3108.

Salati, E. and P. B. Vose (1984). Amazon basin- a system in equilibrium. Science 225(4658): 129-138.

Shukla, J. and Y. Mintz (1982). Influence of land-surface evapotranspiration on the Earth's climate. Science 215: 1498-1501.

Shukla, J., C. A. Nobre and P. J. Sellers (1990). Amazon deforestation and climate change. Science 247(4948): 1322-1325.

Shuttleworth, W. J. (1989). Micrometeorology of temperate and tropical forest. Philosophical Transactions of the Royal Society of London Series B 324: 299-334.

Soil Science Society of America (1997). Glossary of Soil Science Terms 1996. Soil Science Society of America, Madison, WI**:** 138p.

Sollins, P. and R. Radulovich (1988). Effects of soil physical structure on solute transport in a weathered tropical soil. Soil Science Society of America Journal 52(4): 1168-1173.

Sternberg, L. d. S. L., M. Moreira and D. C. Nepstad (2002). Uptake of water by lateral roots of small trees in an Amazonian Tropical Forest. Plant and Soil 238: 151-158.

Thorburn, P. J. and J. R. Ehleringer (1995). Root water uptake of field-growing plants indicated by measurements of natural-abundance deuterium. Plant and Soil 177: 225-233.

Thornthwaite, C. W. (1948). An approach toward a rational classification of climate. Geographic Review 38: 55-94.

Thornthwaite, C. W. and J. R. Mather (1957). Instructions and Tables for Computing Potential Evapotranspiration and the Water Balance. Centerton, Drexel Institute of Technology Laboratory of Climatology, New Jersey**:** 311p.

Tomasella, J. and M. G. Hodnett (1996). Soil hydraulic properties and van Genuchten parameters for an oxisol under pasture in central Amazonia. *In* Amazonian Deforestation and Climate. J. H. C. Gash, C. A. Nobre, J. M. Roberts and R. L. Victoria. John Wiley and Sons, New York**:** 101-124.

Tomasella, J. and M. G. Hodnett (1998). Estimating soil water retention characteristics from limited data in Brazilian Amazon. Soil Science 163(3): 190-202.

Tomasella, J., M. G. Hodnett and L. Rossato (2000). Pedotransfer functions for the estimation of soil water retention in Brazilian soils. Soil Science Society of America Journal 64: 327-338.

Trenberth, K. E. and T. J. Hoar (1996). The 1990-1995 El Nino-Southern Oscillation event: longest on record. Geophysical Research Letters 23: 57-60.

Ubarana, V. N. (1996). Observations and modelling of rainfall interception at two experimental sites in Amazonia. *In* Amazonian Deforestation and Climate. J. H. C. Gash, C. A. Nobre, J. M. Roberts and R. L. Victoria. John Wiley and Sons, New York**:** 151-162.

Uhl, C. and J. B. Kauffman (1990). Deforestation, fire susceptibility, and potential trees responses to fire in the eastern Amazon. Ecology 71(2): 437-449.

van Genuchten, M. T. (1980). A closed-form equation for predicting the hydraulic conductivity of unsaturated soils. Soil Science Society of America Journal 44: 892-898.

Villa Nova, N. A., E. Salati and E. Matsui (1976). Evapotransiração na bacia Amazonica. Acta Amazônica 6: 215-228.

Yang, S. J. and E. de Jong (1972). Effect of aerial environment and soil water potential on the transpiration and energy status of water in wheat plants. Agronomy Journal 61: 571-578.

Zeng, N., W. J. Shuttleworth and J. H. C. Gash (2000). Influence of temporal variability of rainfall on interception loss. Part I. Point analysis. Journal of Hydrology 228: 228-241.

# CHAPTER 3

# MODELING THE EFFECTS OF PARTIAL THROUGHFALL EXCLUSION ON THE DISTRIBUTION OF SOIL WATER IN A BRAZILIAN OXISOL UNDER TROPICAL MOIST FOREST[1]

[1] E. L. Belk, D. Markewitz, T. C. Rasmussen, D. Radcliffe and D. Nepstad. To be submitted to Water Resources Research.

# CHAPTER 3

# MODELING THE EFFECTS OF PARTIAL THROUGHFALL EXCLUSION ON THE DISTRIBUTION OF SOIL WATER IN A BRAZILIAN OXISOL UNDER TROPICAL MOIST FOREST


## Abstract

The tropical moist forests of Amazonia are periodically subjected to severe drought induced by El Niño Southern Oscillation events. Access to water reserves in deep soil during periods of reduced precipitation determines whether or not the forest will be buffered from the deleterious effects of water deficit. Increasing frequency and severity of such drought events, as predicted by some global climate change models, may limit the buffering capacity of these resource reserves leading to tree mortality, changes in forest composition, and greater susceptibility to fire. A model was developed to simulate changes in the distribution of soil water and its effects on nutrient availability within an existing throughfall exclusion experiment located in the Tapajós National Forest, east-central Amazonia (Brazil). Simulations using data from the first 2.5 years of the experiment capture mild soil water depletion near the surface after the first year of treatment, and decreasing soil moisture at depth during the second year. Sensitivity analysis revealed that the water component of the model is most sensitive to the parameters of the water retention and unsaturated flow equations, while the nutrient component is most sensitive to the partition coefficients defining the equilibrium between solution and adsorbed phases. The model may be used to determine whether and how throughfall exclusion from a tropical moist forest affects water and nutrient cycling.

## Introduction

Although tropical rain forests cover less than ten percent of the earth's land surface (Whittaker and Likens 1973), they have a disproportionate importance in the exchange of carbon, water, and energy between the biosphere and atmosphere (Schlesinger 1997). While the function of the Amazon river basin in the global water cycle is well recognized, we are only beginning to understand the interaction of factors affecting the below-ground partitioning and availability of water and nutrients to the vegetation in its forest ecosystems. These processes are important for interpreting how humid tropical forests manage to maintain evergreen canopies during the annual dry season and for predicting how these forests might respond to prolonged periods of drought, such as those that result from El Niño Southern Oscillation (ENSO) events.

To study the response of a humid Amazon forest to severe drought, a partial throughfall exclusion study was initiated in 1998 in the Tapajós National Forest, east-central Amazonia, near Santarém, Brazil (Nepstad et al. 2002; Figure 2.1). This experiment compares two one-hectare plots, one of which receives natural rainfall, while the other has plastic panels installed in the forest understory during the rainy season. These panels capture approximately 60% of incoming throughfall, channeling the water to a system of gutters and diverting it from the soil. Both plots are surrounded by a 1.5-meter deep trench, which reduces the ability of the trees under study to access water from outside the plots. A variety of processes are being monitored, including: tree growth and mortality, sapflow, litterfall, leaf area index, forest floor decomposition, soil respiration, trace gas emissions, forest floor flammability, and the amounts and chemistry of precipitation, throughfall, litter leachate, and soil solutions. Soil moisture content is also

measured by time domain reflectometry (Topp et al. 1980) using soil shafts that allow access to twelve-meters depth in both the exclusion and control plots.

The overall objective of the throughfall exclusion experiment is to understand how tropical forests respond to severe drought. The goal of this project is to provide a physically based model of the soil water dynamics of the study site. Soil moisture measurements alone do not describe the magnitudes and rates of water fluxes because two layers may contain the same volume of water in a given volume of soil, but have different amounts of water flowing through them. A simulation model is proposed to predict whether and how soil water distribution, steady flux between layers, and deep drainage are affected by reduced inputs, in turn affecting the accessibility of water and nutrients to the forest. The throughfall exclusion experiment and its infrastructure provide an excellent opportunity to study soil water dynamics in a deeply weathered tropical soil. Knowledge of the changes in below-ground storage and partitioning of water will enhance the ability of investigators to explain other responses of the forest to drought conditions. By quantifying how the ecological functions of this tropical forest change during prolonged drought, we hope to better understand the more subtle changes that occur during the annual dry season and to predict the ability of these forests to tolerate reductions in precipitation associated with land use conversion or long-term climate change.

## Model Structure

### *Description of Model*

The model was designed to simulate daily changes in the distribution of soil water in a tropical moist forest in Amazonia undergoing experimentally imposed drought.

Vertical water movement through 13 soil layers is driven by the difference in total soil water potential, which integrates the effect of matric and gravitational forces. Fluxes of K and Ca to the soil from throughfall and decomposing litter, adsorption and desorption exchange between solution and solid phases, and leaching of the elements through the top four soil layers are also predicted. Plant uptake of water and nutrients to the forest vegetation is included. Simulations may be performed for the control plot with no reduction in water inputs or for the treatment plot where 60% of throughfall is excluded during the rainy season. A flow diagram of the model is depicted in Figure 3.1.

The model was written using Stella 6.0 Research software (High Performance Systems, Inc., Hanover, N.H.) and uses the Euler method to integrate 24 times each day. Calibration was performed using soil volumetric water contents measured in the control plot during the first 2.5 years of the experiment. When the treatment switch is selected the model will predict soil volumetric water contents for the same time period as the forest undergoes partial throughfall exclusion.

***Required model inputs***

Steady water flow through several layers of the unsaturated zone is simulated. The top boundary is a prescribed flux defined by throughfall inputs while the lower boundary is a prescribed matric potential. Table 3.1 contains a list of the inputs required by the model. The units of the inputs are reported as they function in the model, which reflects the fact that water and nutrient fluxes are simulated only in the vertical direction. Whenever additional dimensions are needed to convert units, the area used is one $cm^2$. Other information about the study site is incorporated into the model implicitly, including

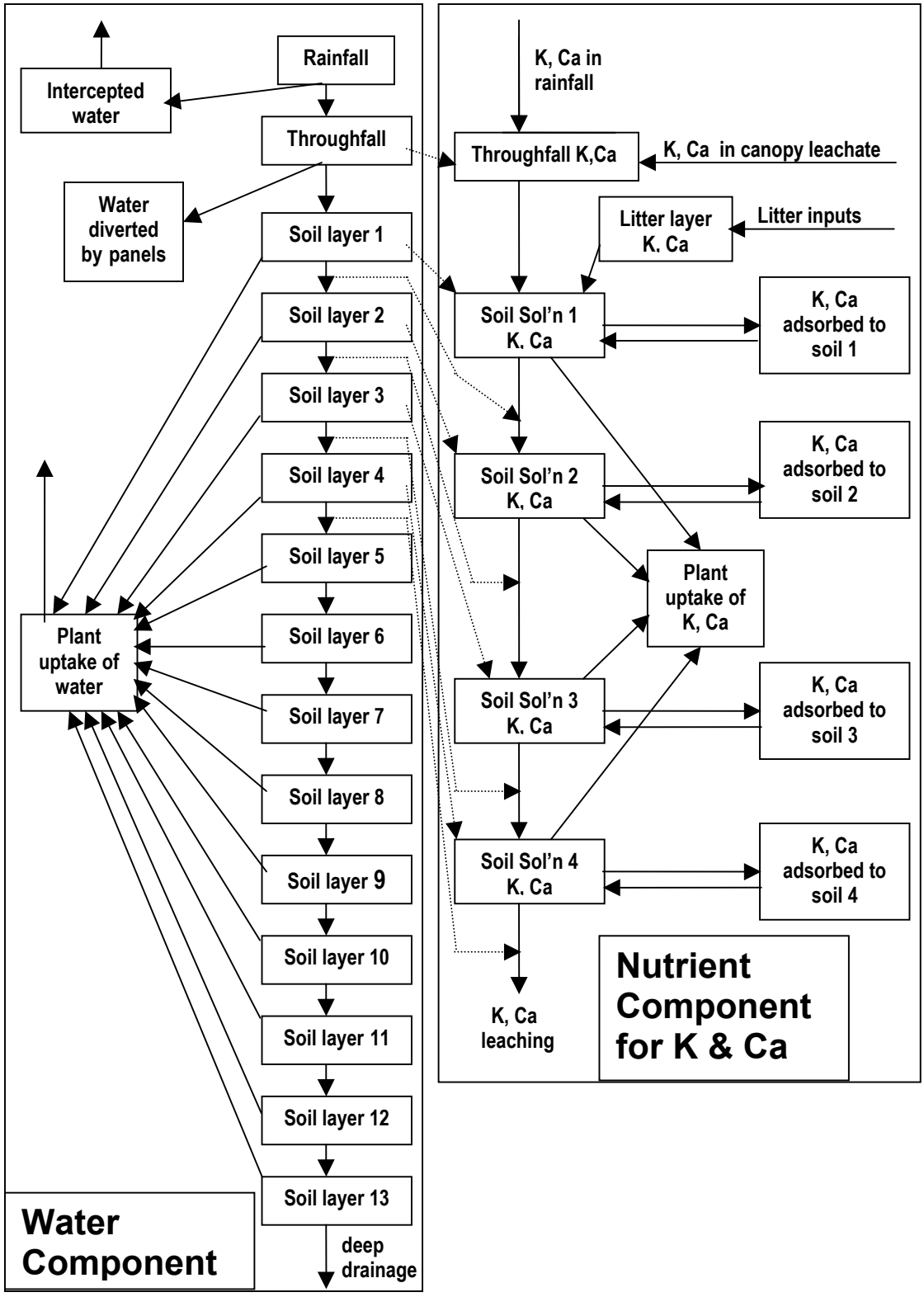


**Figure 3.1 Idealized model structure for water and nutrient cycling in a deep Oxisol. Solid arrows represent fluxes of material and dashed arrows represent transfers of information.**

**Table 3.1 Model inputs. Parameters with (z) are input for each layer of soil.**

| Input | Description | Units |
|---|---|---|
| Rainfall | Daily rainfall depth | cm-$H_2O$ $day^{-1}$ |
| Throughfall fraction | Fraction of rainfall that becomes throughfall (portion that reaches the soil) | unitless |
| ED (z) | Equivalent depth of water in a soil layer | cm-$H_2O$ |
| $\theta_s$ (z) | Van Genuchten parameter for water retention; saturated water content | cm-$H_2O$ $cm\text{-}soil^{-1}$ |
| $\theta_r$ (z) | Van Genucthen parameter for water retention; residual water content | cm-$H_2O$ $cm\text{-}soil^{-1}$ |
| α (z) | Van Genuchten parameter for water retention; shape parameter | $cm^{-1}$ |
| n (z) | Van Genuchten parameter for water retention; shape parameter | unitless |
| $K_{sat}$ (z) | Saturated hydraulic conductivity | cm-$H_2O$ $day^{-1}$ |
| Δ z (z) | Distance from the midpoint of one layer to the next | cm |
| PET | Daily potential evapotranspiration | cm-$H_2O$ $day^{-1}$ |
| R (z) | Fraction of root length or root biomass present in a soil layer | unitless |
| H at depth | Total (head) potential at a known depth | cm |
| Litterfall | Daily amount of litter being added to the forest floor | mg-litter $day^{-1}$ |
| Litter temperature | Temperature of the forest floor litter | ˚C |
| $K_{decomp}$ | Decomposition rate constant for litter | $day^{-1}$ |
| FF | Mass of litter comprising forest floor | mg-litter |
| Daily K/Ca concentration in throughfall | Relationship between throughfall and the concentration of K/Ca expected to be in that amount of water. | mg-K/Ca $cm^{-1}$-$H_2O$ |
| Canopy leaching K/Ca | The fraction of K/Ca in throughfall contributed by canopy leaching (i.e. not from rainfall) | unitless |
| $K_d$ K/Ca | Partition coefficient between solid and solution phases of the element | $cm^3$ $g^{-1}$ |
| K/Ca $C_s$ (z) | K/Ca in each cm of soil solution (for a $cm^2$ area) | mg-K/Ca |
| K/Ca $C_l$ (z) | Readily exchangeable K/Ca adsorbed to particle surfaces per g soil | mg-K/Ca |

the bulk densities of the soil layers, which are used to convert the adsorbed amounts of the elements to concentrations, and the air temperature, which is used to estimate potential evapotranspiration (PET). The depth increments of the 13 soil layers are as follows: 1. 0-40 cm, 2. 40-75 cm, 3. 75-150 cm, 4. 150-250 cm, 5. 250-350 cm, 6. 350-450cm, 7. 450-550 cm, 8. 550-650 cm, 9. 650-750 cm, 10. 750-850 cm, 11. 850-950 cm, 12. 950-1050 cm, 13. 1050-1150 cm (Figure 3.2). These increments were chosen so that the TDR probes would be at or near the midpoints of each layer. Because lysimeters are installed at 25 and 200 cm, nutrient fluxes are simulated only through the top four layers covering 0-250 cm. It is possible to change the depths of the layers, but then the gravitational potentials and flow distances would need to be adjusted accordingly.

***Water inputs to the forest***

Rainfall enters the forest system and is partitioned into throughfall and interception. Throughfall is considered to be any water that reaches the soil, regardless of whether it came into contact with vegetation on the way down. Throughfall is set at 88% of incoming rainfall, with the balance (12%) being intercepted by the canopy. These percentages were empirically established from data relating the average rainfall at 3 gauges located in and near the study site to the throughfall volumes collected in both plots (Figure 3.3). The same throughfall fraction is used year-round, as the relationship did not vary significantly by seasons (at least within our ability to measure those volumes).

The model contains a switch to allow selection of simulating the treatment or control plot. With control plot selected, all throughfall enters the soil. When the

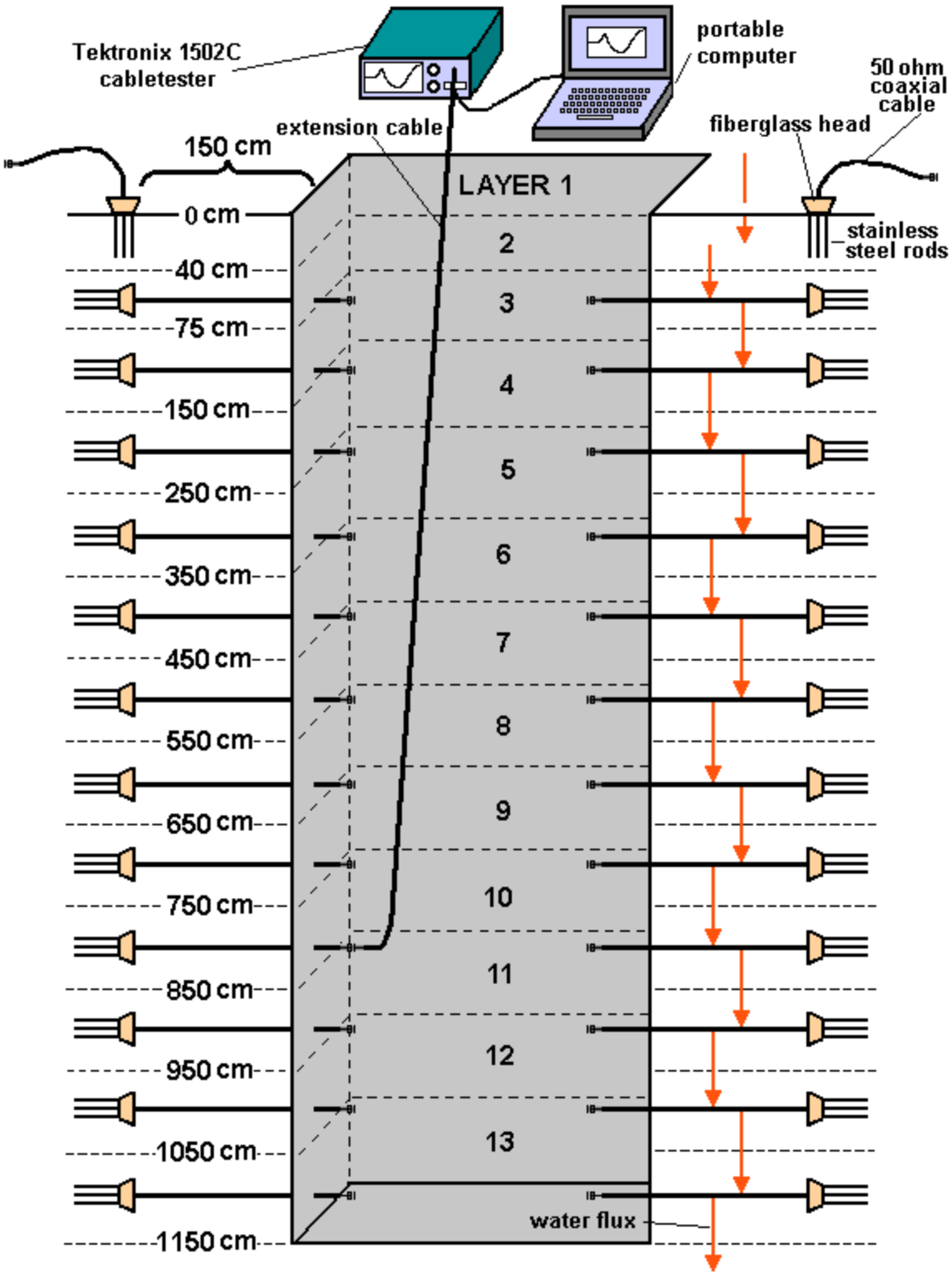


**Figure 3.2 Installation of triple-wire TDR sensors in opposite walls of deep soil shafts, Tapajós National Forest, Brazil. Auger holes for installation are back-filled with soil to pit wall. A constant length of 50 ohm coaxial cable is used to connect between each probe cable and the cabletester. Dashed lines mark model layer boundaries and arrows depict water flow from layer midpoint to midpoint.**

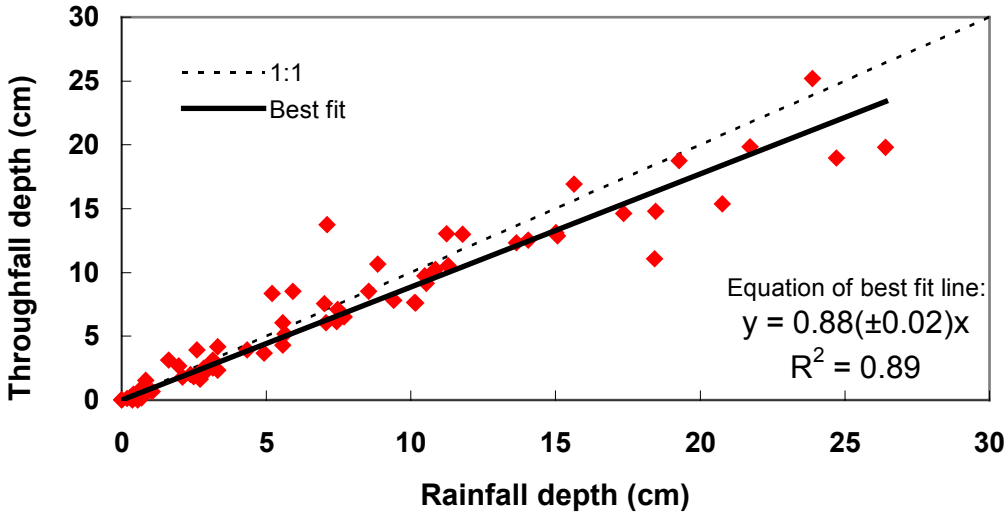


**Figure 3.3 Relationship between rainfall and throughfall for the Tapajós National Forest, south of Santarém, Pará, Brazil. Rainfall is an average of three collectors while throughfall is an average of 20 collectors. Data is from the period May 1999 to December 2001.**

treatment plot is selected, 60% of throughfall water is diverted from the soil during the time periods when the panels were in place. The estimate of the panel effect is based on measurements of water collected into the gutters during several rainstorms (D. Nepstad unpublished data).

***Soil Water***

Throughfall infiltrates directly into the soil at the first layer. All thirteen layers hold a depth of water (ED, in cm) equivalent to the soil moisture in their increment of soil. The ED of water in each layer is initialized with soil water content data from May 17, 1999, the first day of simulation. The water content of a layer ($\theta$; $cm^3$-water $cm^{-3}$-soil) may then be determined by knowing the ratio between the depth of water (cm) in that thickness of soil (L; cm):

$$\theta(z) = \frac{ED(z)}{L(z)} \qquad [3.1]$$

Steady water fluxes moving between layers are determined by an extension of Darcy's equation for one-dimensional (vertical), unsaturated flow (Muller 1999):

$$q = K(\theta) \times \left[ \frac{\Delta H}{\Delta z} \right] \qquad [3.2]$$

where q is the steady water flux (cm $day^{-1}$), $K(\theta)$ is the unsaturated hydraulic conductivity (cm $day^{-1}$), $\Delta H$ is the difference in total potential between two adjoining layers (cm) and $\Delta z$ is the distance for flow between the midpoints of the layers (cm). The total potential of the soil water, H, in a given layer is the sum of the matric ($h_m$) and gravitational ($h_z$) potentials:

$$H(z) = h_m + h_z \qquad [3.3]$$

The matric potential of the soil water is determined by the van Genuchten equation relating water content to potential (van Genuchten 1980):

$$h_m = \left( \frac{1}{\alpha} \left( \Theta^{\frac{-1}{m}} - 1 \right)^{\frac{1}{n}} \right) \qquad [3.4]$$

where Θ is the relative saturation of the soil ($cm^3$-water $cm^{-3}$-soil) equal to:

$$\Theta = \frac{\left(\theta - \theta_r\right)}{\left(\theta_s - \theta_r\right)} \qquad [3.5]$$

and α ($cm^{-1}$), n and m are fitting parameters. The parameter m is taken to be 1-1/n. The soil surface serves as the datum where gravitational potential is zero so $h_z$ is equal to the difference in the elevation of the layer midpoint with respect to the datum, i.e. $h_z$=z, where z is the (negative) distance of the layer midpoint below the soil surface (cm). Unsaturated hydraulic conductivity, K(θ), is calculated from saturated hydraulic conductivity, $K_{sat}$, values according to the equation (Mualem 1976):

$$K(\theta) = K_{sat} \left( \frac{\theta - \theta_r}{\theta_s - \theta_r} \right)^{0.5} \left( 1 - \left( 1 - \left( \frac{\theta - \theta_r}{\theta_s - \theta_r} \right)^{\frac{n}{n-1}} \right)^{m} \right)^2 \qquad [3.6]$$

***Water flux out of the system***

Deep drainage (cm $day^{-1}$) out of the lowest layer is calculated following Darcy's equation assuming that the matric potential at 125 m depth is 0 (i.e. the soil is saturated so $h_m = 0$). Therefore, the total potential equals the gravitational potential ($H = h_z = z$).

***Plant uptake of water***

Water required for transpiration by vegetation (cm $day^{-1}$) is removed from each soil layer before downward percolation is allowed. It is assumed that when a vapor

pressure deficit between the forest and surrounding atmosphere exists, water will evaporate from vegetative surfaces more readily than it can be transpired through leaf stoma. Intercepted water is first used to satisfy evapotranspirational demand, which is determined by the potential evapotranspiration (PET). Intercepted water is temporarily stored on the canopy and allowed to evaporate directly from it at a rate up to the PET. If more water is intercepted than can be potentially evapotranspired, then no water is taken from the soil during that time step. When the PET is greater than the amount of water stored on the canopy, then water is taken up from the soil in an amount equal to the difference. The fraction of this total uptake extracted from a given layer is:

$$U(z) = U_{max}\, R(z)\, URF(z) \qquad [3.7]$$

where $U_{max}$ is the maximum amount of water extracted from the soil (cm), R(z) is the proportion of fine root biomass in a given layer and URF(z) is a factor that restricts plant uptake based on the matric potential, which indicates the amount of energy required to remove water from the soil (Figure 3.4). The URF factor used in the model is similar to other uptake reduction functions based on potential except that h3, which defines when soil moisture is low enough to limit uptake, does not vary with PET, and uptake near saturation is not restricted (Feddes et al. 1978; Feddes et al. 2001).

A modified version of the Thornthwaite model was chosen to estimate potential evapotranspiration (PET) because it requires fewer data inputs (only monthly air temperature and site latitude). The modification is the inclusion of a factor to correct the tendency of the original Thornthwaite model to overestimate PET when average air temperature is greater than 26.5ºC (Amorim et al. 1999). The monthly PET estimates are then partitioned into equal daily fractions to be consistent with the daily time

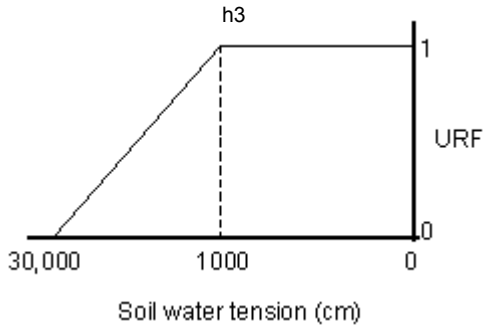


**Figure 3.4 Uptake reduction factor, URF, used to restrict plant uptake of soil water from a layer based on its matric potential. The point h3 defines when plant uptake is restricted due to limited soil moisture. The function is modified from Feddes et al. (2001).**

specifications of the model. The Thornthwaite calculations are performed independent of and prior to model simulation and are then provided as a daily input for simulation. Obviously, this method fails to capture daily variation in PET, but the water content outputs are validated on an approximate monthly basis.

***Input of elements to and leaching through the soil***

Potassium (K) and calcium (Ca) are transported to the soil by litterfall and throughfall. The daily litterfall (including leaves, twigs <1 cm diameter, and reproductive parts) was estimated from bi-weekly collections as part of the throughfall exclusion experiment (Nepstad et al. 2002; see also Figure 3.5). Litterfall for 2001 was not yet published, so those values were assumed to be the same as 2000. Litter is decomposed according to first order kinetics:

$$OM_{release} = K_{decomp}\, FF\, (TRF*MRF)^{0.5} \qquad [3.8]$$

where $OM_{release}$ is the organic matter released through decomposition, $K_{decomp}$ is the rate of litter decomposition, FF is the stock of litter accumulated on the forest floor and TRF and MRF are temperature and moisture restriction factors that reduce the decomposition rate for temperature or moisture conditions outside the optimum range. The geometric mean of the temperature and moisture factors is used because it is assumed that there is some interaction in their effects. The decomposition rate is interpolated from litter sample data presented in Nepstad et. al. (2002) for the average percent mass remaining in large mesh screen bags placed on the forest floor in the control plot over a period of eight months.

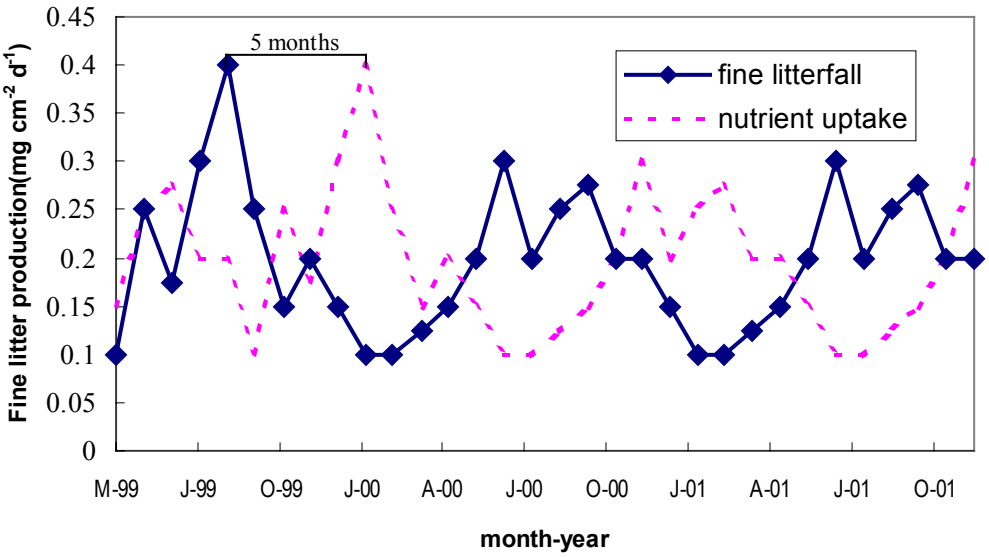


**Figure 3.5 Fine litter production, including foliage, flowers, and fruits, and nutrient uptake due to leaf growth in the Tapajós National Forest, Brazil. Fine litter production rates were extrapolated from data published in Nepstad et al. (2002). The nutrient uptake function incorporates a five-month lag of the litter production data, following the steady state assumption that nutrients lost in litterfall must be replaced for the growth of new leaves and flowers to occur.**

The temperature of the litter is assumed to be similar to air temperature measured under the canopy. Since the decomposition rate used was not an estimate of the maximum but rather the actual observed rate, the temperature factor in the model is modified from Parton et al. (1987) so that the factor is at unity around 25ºC, which is the average temperature of the litter (Figure 3.6a). The moisture factor is based on the ratio of the water content of the top layer of soil (θ) to the porosity (φ) of that layer (which would be the saturated water content when all pores are full of water). The moisture factor is 1 when the ratio of pores full of water to available pore space is 50-60% because that is usually when maximum biological activity occurs (Paul and Clark 1996; Figure 3.6b). Once litter decomposition is calculated, the K and Ca added to the soil is 0.34% and 1.7% of the decomposed material, respectively (D. Markewitz unpublished data).

Throughfall fluxes of K and Ca are estimated by a function relating daily throughfall inputs to the concentration of each element in the throughfall volume (Figure 3.7). Nutrients are leached through the soil in the same proportion as the water fluxes move water out of the layers.

***Adsorption and Desorption***

Exchange between ions adsorbed to the surfaces of soil particles and ions in solution is known to be fast (on the order of hours) in kaolinitic soils (Barber 1995). The relationship between the concentration of K or Ca adsorbed to the soil ($C_s$) and K or Ca in soil solution ($C_l$) is assumed to be linear for the range of concentrations encountered in this study:

$$C_s = K_d C_l \qquad [3.9]$$

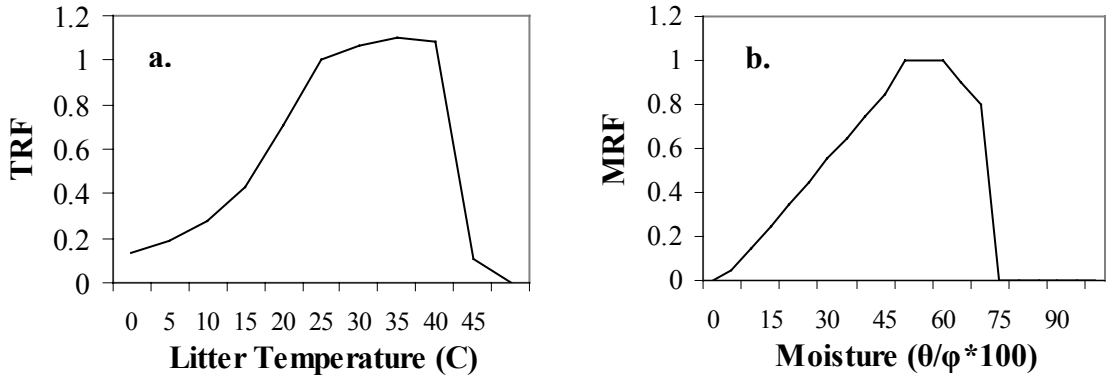


**Figure 3.6 a.) Temperature and b.) Moisture factors to restrict the litter decomposition rate due to sub-optimal conditions. The temperature factor is modified from Parton et al. (1987) and exceeds one because the decomposition rate used in the model is the observed, not the maximum rate. The moisture factor is based on the assumptions that the humidity of the litter is similar to that of the top soil layer and that maximum microbiological activity occurs when the ratio of water-filled pores to available pore space (θ/φ) is 50-60% (Paul and Clark 1996).**

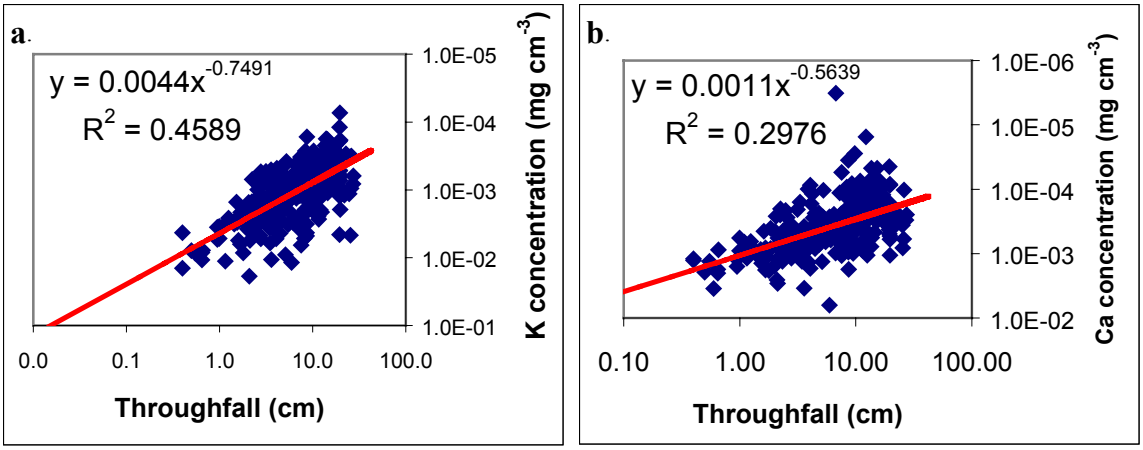


**Figure 3.7 Daily throughfall inputs versus K and Ca concentrations in the Tapajós National Forest, Brazil. Throughfall is sampled bi-weekly from 10 collectors in the control plot. Data are from the period May 1999 to July 2001 and are fit with power functions used to predict concentrations of K and Ca from throughfall.**

where $C_s$ is the concentration in the solid phase (mg g-soil$^{-1}$), $C_l$ is the concentration in the liquid (solution) phase (mg cm$^{-3}$-water), and $K_d$ is the partition coefficient. The $K_d$ values are taken from Sheppard and Thibault (1990) for clay soils ($K_d$ = 75 cm$^3$ g$^{-1}$ for K and 50 cm$^3$ g$^{-1}$ for Ca). As elements are added to and removed from the soil, the model maintains equilibrium between the pools of adsorbed and solution K and Ca by moving the element from one pool to the other so that the ratio of $C_s$ to $C_l$ remains equal to $K_d$.

***Plant uptake of nutrients***

While the model drives uptake of water by evaporative demand, plant uptake of elements is driven by the need to replace nutrients lost in fallen leaves and those leached from the canopy. Therefore, plant uptake of K and Ca is estimated from litterfall and canopy leaching. The litterfall rates, which tend to be highest in around August or September, were lagged by about 5 months so that the greatest uptake of nutrients due to leaf loss would be around January or February, which is when LAI, stemwood production, and fruiting peak (Nepstad et al. 2002; Figure 3.5). The fraction of nutrients in throughfall that were contributed by canopy leaching (as opposed to rainfall) was determined by comparing rainfall and throughfall flux data reported in Markewitz et al. (in press). The K in throughfall is roughly ten times greater than the K in rainfall, so it is estimated that about 10% of the K in throughfall comes from the rain and the balance 90% was leached from the canopy. For Ca, it was estimated that only 60% of throughfall nutrients are from canopy leaching.

### *Assumptions in the Model*

During model development, a number of simplifying assumptions were made:

1. Throughfall is consistently 88% of rainfall.
2. The litter layer of the soil does not delay or store throughfall.
3. There is no evaporation from the soil surface.
4. There is no lateral movement of water in the soil.
5. Water fluxes are steady and there is no preferential flow.
6. Saturated hydraulic conductivity at depth decreases according to the power function $y = 58x^{-0.9}$ fit to field data from the upper four meters.
7. The soil at 125 m depth is saturated ($h_m$=0).
8. In satisfying atmospheric demand for water vapor, water intercepted by the canopy evaporates first before water is taken up from the soil by roots.
9. Water uptake from a given layer can be described by the fine root distribution and soil water potential.
10. The fine root distribution does not change and the root biomass in a layer is evenly distributed through the soil such that water (at the same potential) and nutrients are equally available.
11. Sorption is instantaneous and reversible.
12. Total plant uptake of nutrients equals the amount of nutrients lost in canopy leaching and litterfall; uptake from layers is partitioned by the root distribution.
13. Litter decomposition is described by first-order kinetics.
14. Canopy leaching is constantly the same percentage of throughfall.
15. Nutrient dynamics is modeled without including the processes of dry deposition, release from mineral weathering, and exchange with organics.

The first assumption was made after attempts to compare measured rainfall with measured throughfall failed to find a difference between seasons or by rainfall amounts. Since rainfall is measured daily (except on weekends), and throughfall is collected bi-weekly, rainfall intensities are not known and cannot be compared to throughfall.

Stemflow is not separated for either the water or nutrient submodels because the design of the experiment being modeled does not exclude it. Although stemflow is disproportionately enriched with nutrients, it does not represent a major contribution of water (Klinge et al. 2001). The relatively high correlation ($R^2 = 0.89$) between rainfall and throughfall is consistent with the fact that the percent coverage of the canopy, which is usually around 95%, did not change by more than a few percent during the time period being simulated (Nepstad et al. 2002). However, as the throughfall exclusion continues the trees will likely display more signs of stress and the canopy coverage may change, in turn affecting the partitioning of rainfall into throughfall and interception.

Throughfall is allowed to infiltrate directly into the soil as it arrives because the litter layer of the site is thin (about 2-4 cm) and the measured surface infiltration rates are high (>200 cm $day^{-1}$). The third assumption is supported because only about 1% of solar radiation penetrates the forest canopy (Nepstad et al. 1996; Nepstad et al. 2002). Other researchers have reported that direct evaporation from the soil surface is negligible in Amazon forests (Jordan and Heuveldop 1981; Salati and Vose 1984).

The locally flat topography and absence of a hardpan or clearly restrictive layer in the upper twelve meters of soil suggests that water flow in these soils is predominantly vertical. Additional support for this assumption is provided by a study of plant water uptake that was conducted at the same site (Sternberg et al. 2002). In the study, the plots were irrigated with deuterated water, and then soil water and plant samples were analyzed for the presence of the deuterium label. Based on these results the authors concluded that was very little horizontal movement of the deuterium.

The Mualem equation used to describe the unsaturated hydraulic conductivity function in the model best predicts capillary flow of water (Mualem 1976). If the soil has developed a structure involving continuous macropores, water may infiltrate faster and deeper than predicted by the equations by bypassing most of the total cross-sectional area of the soil. Certainly, old root channels and animal burrows complicate water flow, especially in the upper meter of the soil profile. The Mualem equation for hydraulic conductivity is anchored by empirical values at saturation (i.e. $K_{sat}$). Field measurements of $K_{sat}$ reflect the effects of macropores on saturated water flow (as long as the sample volume is large enough to include representative macropores), but in using $K_{sat}$ to anchor the equation, unsaturated flow at the wet end of the $K(\theta)$ function may be overpredicted. A deuterium study conducted at a Paragominas forest site with Oxisols similar to the ones at the throughfall exclusion study site found that labeled water inputs displaced water already present in the soil instead of mixing with it (Moreira et al. 2000). This may mean that, over the 12-meter soil profile, preferential water movement is not important.

The saturated hydraulic conductivity ($K_{sat}$) values used in the model for 0 to 400 cm were measured with a Guelph permeameter (Figure 3.8). Below that, the values were estimated by a power function fit to the measured data. $K_{sat}$ is a highly variable soil property that may vary by orders of magnitude even for measurements made near each other and $K_{sat}$ may also differ for the same sample depending on the method used to measure it (Klute and Dirksen 1986; Hillel 1998). Since most studies of $K_{sat}$ are limited to the upper meters of soil, it is not known whether using a power function to predict $K_{sat}$ at depths greater than 4 meters is reasonable. However, it does seem reasonable to

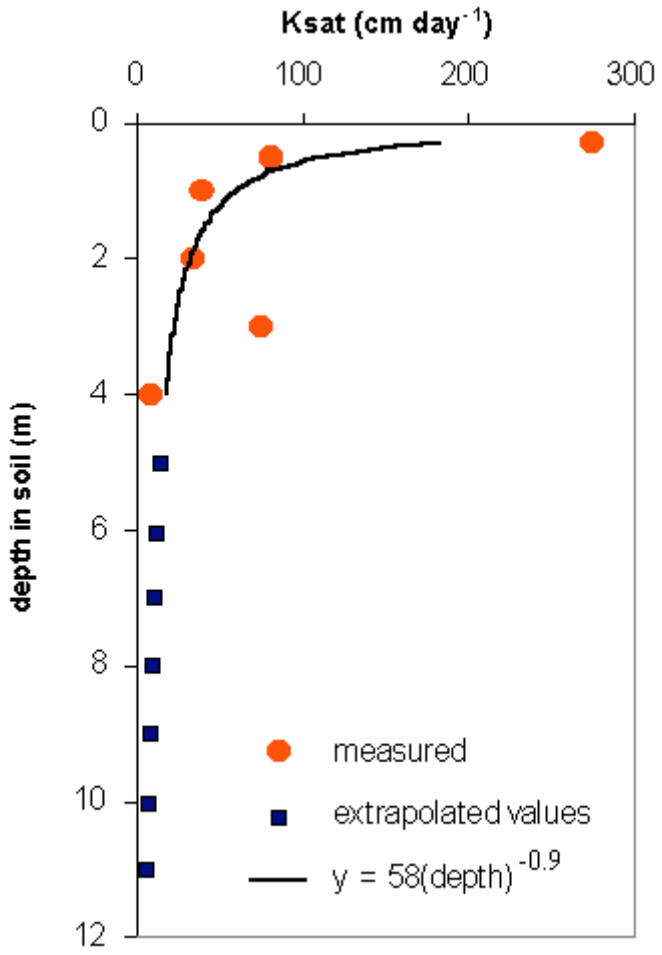


**Figure 3.8 Saturated hydraulic conductivity, $K_{sat}$, in the Tapajós National Forest, Brazil as a function of depth in the soil. The $K_{sat}$ values from 0-4 m were measured with a Guelph permeameter and values below that were extrapolated from a power function fit to the measured data.**

assume that $K_{sat}$ decreases with depth, since it is highly affected by total porosity and the soil becomes less structured with depth.

The seventh assumption, that saturated conditions persist at 125 m depth (and that therefore the matric potential is zero there), seems reasonable given that the water table is below 100 meters deep at the site (Nepstad et al. 2002). The lower boundary conditions will have some effect on the simulated drainage rate out of the lowest layer, but will have less of an influence on the water content of the profile overall. In the model, intercepted water is stored in the canopy and evaporated as the PET allows. Vegetation does not take up water from the soil until the canopy is dry. While this assumption may not be entirely realistic, it has been shown that water stored on leaves evaporates more readily than water transpires through leaf stoma (Ubarana 1996).

Plant uptake is reduced from PET by a factor that assumes water held at tensions above 1,000 cm is relatively free to move and be taken up while water held at tensions greater than 30,000 cm is not (Figure 3.4). Between 1,000 cm and 30,000 cm tension uptake is reduced linearly. In clayey Brazilian Oxisols, most available water is held at tensions above about 1,000 cm (100 kPa; Tomasella and Hodnett 1998). While the permanent wilting point below which vegetation cannot theoretically extract water is usually considered to be a tension of 15,000 cm, Jipp (1998) frequently measured dry season water contents corresponding to tensions above that under a mature Amazon forest.

The fraction of fine root biomass in a soil layer is used to distribute plant uptake between the layers. The underlying assumption is that the presence of roots indicates that they are actively extracting water and nutrients, but some studies have shown that this is

not always true (Ehleringer and Dawson 1992; Moreira et al. 2000). The model lacks a mechanism to account for a change in the distribution of fine roots. Fine root biomass down to six meters at this site was first estimated in August 2000 as part of the throughfall exclusion study. In July 2001, over two years after the start of the experiment and about one and one-half years after the treatment panels were first installed, a second series of root sampling was performed, but only from 0-2 meters (where most of the soil moisture depletion had occurred). The results show no significant difference in root biomass between the treatment and control plot (D. Nepstad unpublished data). However, because deeper depths were not sampled, it is not known whether and how the root biomass changed below 2 meters. As the surface layers continue to dry out, fine root growth at depth is hypothesized (Nepstad et al. 2002).

Allowing adsorption and desorption to occur within one daily time step is appropriate given that exchange between ions adsorbed to particle surfaces and ions in solution is known to occur within hours in kaolinitic soils (Barber 1995). Nutrient cycles in mature Amazon forests are generally thought to be close to steady state (Jordan 1982; Markewitz et al. in press), so on an annual basis it may be reasonable to assume that the uptake of an element is approximately equal to the recycling of that element from canopy leaching and litterfall. The model does not include the processes of nutrient release from minerals or other non-readily exchangeable forms. It also does not explicitly account for dry deposition of elements as inputs to the system, although they may be washed in with wet throughfall deposits because the collectors are left in the field. Salati and Vose (1984) report that natural concentrations of elements in aerosols are low (less than 10 μg $m^{-3}$ air), with K, Ca and other cations constituting a small fraction of the aerosols.

However, they also noted that aerosols may be important inputs in areas where burning is occurring. The soil at this site has low organic matter content and is already highly weathered (Markewitz et al. in press). Nutrient balances have found that losses are equal to or less than inputs, which suggests that most of the nutrient recycling in the Amazon basin is from rainfall, litter and canopy leaching, and not from mineral weathering (Jordan 1982). Litter decomposition is described by first-order kinetics, which implicitly assumes that the rate is proportional to the amount of substrate but not on microbial biomass populations.

## Materials and Methods

### *Research Site*

The forest being modeled is located in a protected area of national forest, the Floresta Nacional Tapajós, east-central Amazonia, south of the city of Santarém do Pará (2.89°S, 54.95°W). The site is about 10 km east of the Tapajós River, but about 90 m above the water level of the river (Nepstad et al. 2002). The soil is an Oxisol (Haplustox) dominated by kaolinite clays, and supports a *terra firme* forest with a continuous canopy around 30-m tall. The term *terra firme* refers to the dense, humid, evergreen forests of the Amazon region that do not flood annually. The throughfall exclusion experiment compares two one-hectare plots, one of which receives natural rainfall, while the other has plastic panels installed in the forest understory during the rainy season. The panels were first installed at the beginning of the 2000 rainy season, following a one-year pretreatment period. When in place, the panels divert approximately 60% of incoming throughfall from the treatment plot. Both plots are surrounded by a 1.5-meter deep

trench, which reduces the ability of the trees under study to access water from outside the plots. The steady water flux model incorporates data collected as part of the throughfall exclusion experiment.

***Soil Moisture***

The volumetric water content ($cm^3\ cm^{-3}$) measurements used to calibrate and quality-check the model were performed with Time Domain Reflectometry (TDR) sensors installed to 11 meters depth in six soil shafts (3 shafts per plot; n = 6 per depth for both plots; Figure 3.2). TDR measurements are made with a cable tester (Textronix 1502C, Beaverton, OR.), which sends an electromagnetic wave down a sensor embedded in the soil (Topp et al. 1980). The travel time of the signal over the length of probe in contact with the soil is determined, and the soil's average dielectric is calculated. The TDR sensors used in this study consist of three, parallel, 24-cm stainless-steel rods (Zegelin et al. 1989). In each deep soil shaft, two TDR sensors are installed horizontally at each meter increment. Each of the six shafts also has two probes installed vertically from 0 to 30 cms, and two probes installed horizontally at 50 cms. Since the shafts are left open to maintain access to the soil profile for root and nutrient studies, the sensors are installed into the undisturbed soil at the end of holes augered 1.5-m into the shaft walls, and the holes are back-filled with soil. Based on a previous study of $CO_2$ concentrations at varying distances inward from the walls of similar open shafts installed in Oxisols in Paragominas, Pará, we believe that the potential drying effect of air within the shaft mixing with soil air 1.5 m into the pit wall is not large (Davidson and Trumbore 1995). The waveforms from these sensors are collected approximately once per month and the

water contents are calculated using an empirical equation developed for mineral soils (Topp et al. 1980), which has been shown to effectively describe the relationship between permittivity and volumetric water contents for surface and deep Oxisols in the Amazon (Jipp et al. 1998).

### *Saturated Hydraulic Conductivity*

Saturated hydraulic conductivity ($K_{sat}$) was quantified with a Guelph permeameter (Soil Moisture Corp., Santa Barbara, CA). Seven surface measurements were made in random locations around the plots using a pressure infiltrometer attachment. The pressure infiltrometer is a 20 cm-diameter ring that can be used to measure the steady state rate of fall of water infiltrating at the soil surface under a constant head (SoilMoisture Equipment Corporation 1986). Additional $K_{sat}$ measurements were made at 0.15, 0.30, 0.5, 1, 2, 3, and 4 m by excavating cylindrical well holes of 6 cm diameter to those depths. Three complete series were completed at each of three sites in the study area. Well holes were gently brushed before measurements to break up any smearing of the clays that occurred during augering.

The $K_{sat}$ results from 0 and 30 cm were averaged and considered to approximate saturated flow rates in the first model layer. The other field measurements were assigned to the closest layer midpoint, and a power function was fit through the points (Figure 3.8). By extending the power function to 11 m, point estimates of $K_{sat}$ were available for the other layers.

### *Rainfall and Throughfall*

Rainfall is input as the average cm $day^{-1}$ collected from three wedge-shaped gauges located in and near the study site. Rainfall is monitored daily, except over the weekend (the Monday values include rain that fell over the weekend).

Rainfall and throughfall samples used in chemical analysis are captured into 16-cm diameter funnels that empty into acid-washed plastic bottles. Each plot has one rainfall collector placed above the canopy and ten throughfall collectors under the canopy. The sample volumes are measured every two weeks, at which time sub-samples are taken for chemical analysis. After each sampling the 10 collectors in each plot are randomly re-assigned a location within the sampling grid for that plot.

### *Nutrients*

Litter leachate solutions are collected by zero-tension lysimeters consisting of 30 x 9 cm PVC troughs buried under the forest floor litter. One lysimeter is located near each of the three deep soil pits per plot. Water that falls into a trough collects into an acid-washed plastic bottle. Tension lysimeters are installed at 25 and 200 cm to collect soil water from each deep soil pit.

All collection bottles are emptied every two weeks and the volume they collect over that time is measured. The samples are then filtered through 0.4 μm polycarbonate filters and placed in cold storage for later chemical analysis. Conductivity, pH and alkalinity are measured, and the samples are analyzed for several elements (including K and Ca) by ion chromatography (Dionex DX 500, Sunnyvale, CA; Clesceri 1998).

***Roots***

The throughfall exclusion experiment generated fine root biomass data (kg-roots $m^{-2}$-soil) from 384 samples (24 borings at eight depths in each of two plots). Each sample was washed and sorted into live and dead fractions, and then sorted into size classes 0-0.99 mm and 1-1.9 mm. The depths at which samples were collected were: 0, 0.50, 1, 2, 3, 4, 5, and 6 m. The root factor for each model layer, R(z), is based on the fraction of the total fine (live) root biomass (0-2 mm) in that layer. For estimating root factors between 6-11 m, the root biomass was considered to be 10% less than in the horizon above.

***Water Release Curves and van Genuchten parameters***

Soil water retention data were generated by the EMBRAPA-CPATU lab in Belém, Pará, Brazil (E. Maklouf unpublished data). A standard pressure plate method was used whereby intact soil cores (n = 4 per depth) are saturated and the water extracted by the application of a steady, constant pressure (Klute and Dirksen 1986). The pressure applied to a soil sample by the pressure plate is considered equal to the suction that must be applied to the soil (by plants or capillary forces) to draw water from it. Samples are weighed after reaching equilibrium at each pressure so that their water contents can be determined gravimetrically. A spreadsheet program was developed to fit van Genuchten soil moisture characteristic (SMC) functions to the data following the procedure outlined in Wraith et al. (1993) for nonlinear estimation by minimizing the sum of squared error terms. The process requires starting with a set of initial values for each parameter, which

are improved by successive iterations. The starting values used were the average $\alpha$, $\theta_s$, $\theta_r$, and n reported by Hodnett and Tomasella (2002) for tropical clay soils.

***PET and associated Meteorological data***

Potential evapotranspiration was calculated using the Thornthwaite method, which provides monthly estimates based on average monthly air temperature (Thornthwaite 1948; Thornthwaite and Mather 1957). The PET values are adjusted for the number of daylight hours in a month based on the site latitude and a factor is applied to correct the tendency of the Thornthwaite model to overestimate PET when average air temperature is greater than 26.5°C (Amorim et al. 1999). The monthly estimates of PET are divided into equal daily values to be consistent with the time step of the water model. Daily daytime air temperatures collected at the canopy level of the control plot were recorded by Hobo dataloggers (Onset Computer Corp., Bourne, MA.), and then averaged for each month.

***Analyses of Model Performance***

The model was calibrated by iteratively changing the van Genuchten (VG) parameters for each layer until the Root Mean Square Error (RMSE) between the measured and simulated volumetric control plot water contents for all depths and all dates was minimized. Sensitivity analyses were performed on the saturated hydraulic conductivity ($K_{sat}$), VG parameters ($\alpha$, $\theta_s$, $\theta_r$, and n ), PET and throughfall fraction. The parameter of interest was assigned at least five other values while the other parameters were left unchanged. The sensitivity of the model to these changes was quantified by

evaluating their effect on the average depth of water stored in that layer, layers above or below, and/or the average depth of water in the entire profile. For some tests, the cumulative plant uptake over the 960-day simulation period was also evaluated. In addition, a full factorial analysis of the $\theta_s$, $\theta_r$, and n from the fourth layer, which extends from 150-250 cm, was completed. Sensitivity analysis of the nutrient component tested the effect of changing the partition coefficients (for both K and Ca) on the average concentration of those elements in solution and the leaching of the element below 250 cm. The effect of the litter decomposition rate constant on the introduction of elements to the soil was also analyzed.

During calibration and sensitivity analysis, it became apparent that the model is unstable when there are large changes in the VG parameters between layers because this may cause one or more layers to wet up or dry down beyond their ranges of validity. A layer will also oversaturate when its maximum flow rate ($K_{sat}$) is too low to accommodate water inputs from daily rainfall or overlying layers. The VG parameters have intrinsic limitations. For example, $\theta_s$ must be greater than $\theta_r$, and should be less than or equal to the total porosity. The parameter $\theta_r$ must be less than $\theta_s$ but not less than zero. The parameter n must be greater than 1. With the current values, the model is unstable if the time step (dt) is larger than 0.1 (1/10) day.

Model performance was evaluated using the mean difference, RMSE, RRMSE and the coefficient of determination ($R^2$) between measured and predicted volumetric water contents. In general, low RMSE and RRMSE and a high $R^2$ indicate good predictions.

## Results and Discussion

### *Calibration*

Most of the values used as input variables or constants were determined by measurements made at the site (Table 3.2). Since the model was unstable when the van Genuchten (VG) parameters fit to laboratory-generated water retention data were used, the model was calibrated for the control plot by changing the VG parameters until the root mean square error (RMSE) between the measured and predicted volumetric water contents for all depths over all dates was minimized. The resulting RMSE is 1.88% water content, which is a relative root mean square error (RRMSE) of 5.1%. However, the standard errors of the six TDR measurements at each depth are typically around 1% water content. The top two layers have poorer fits than the others, with RRMSEs of 10% or greater. Excepting the third layer, which has an RRMSE of 5.4%, the errors in the other horizons are all below 4.6%. The poorer fit in the top horizons, which have greater spatial variability than deeper layers, may also be due to hysteresis in the soil moisture characteristic functions (SMC). Hysteresis refers to the phenomenon whereby the relationship between water content and water potential (i.e. the SMC) varies depending on whether the soil is wetting or drying. While the calibrated soil moisture characteristic functions probably represent an intermediate fit between the wetting and drying curves, the error in describing this function with one set of parameters is greater where the soil moisture conditions are more dynamic, such as they are in the upper soil layers.

Figure 3.9 shows the field-generated TDR data versus the model simulations of water content. The calibrated model captures important seasonal trends and shows the expected delay in recharge and depletion responses with increasing depth. The timing of

**Table 3.2a Parameter values and initial values for stocks input for each model layer. Note that the initial concentrations of K and Ca in soil solution are zero.**

| Layer | Depths (cm) | Initial ED Control (cm $H_2O$)[1] | Initial ED Treatment (cm $H_2O$)[1] | $\theta_s$ ($cm^3$ $cm^{-3}$)[2] | $\theta_r$ ($cm^3$ $cm^{-3}$)[2] | $\alpha$ ($-cm^{-1}$)[2] | n (unitless)[2] | $K_{sat}$ (cm $H_2O$ $day^{-1}$)[3] | R (unitless)[4] | K adsorbed to soil (mg K)[5] | Ca adsorbed to soil (mg Ca)[5] |
|---|---|---|---|---|---|---|---|---|---|---|---|
| 1 | 0-40 | 15.5 | 12.5 | 0.44 | 0.24 | 0.040 | 1.2 | 273.8 | 0.688 | 0.8148 | 0.9004 |
| 2 | 40-75 | 10.6 | 10.9 | 0.41 | 0.23 | 0.040 | 1.5 | 77.6 | 0.103 | 0.2626 | 0.2014 |
| 3 | 75-150 | 24.7 | 22.5 | 0.40 | 0.21 | 0.040 | 1.5 | 37.6 | 0.050 | 0.8885 | 0.2030 |
| 4 | 150-250 | 33.9 | 30.7 | 0.35 | 0.20 | 0.055 | 1.3 | 33.3 | 0.030 | 0.9854 | 0.2020 |
| 5 | 250-350 | 37.0 | 32.5 | 0.46 | 0.22 | 0.050 | 1.5 | 73.4 | 0.022 | - | - |
| 6 | 350-450 | 37.8 | 35.4 | 0.44 | 0.23 | 0.055 | 1.6 | 7.4 | 0.019 | - | - |
| 7 | 450-550 | 41.5 | 37.4 | 0.47 | 0.23 | 0.050 | 1.4 | 14.2 | 0.019 | - | - |
| 8 | 550-650 | 42.3 | 39.4 | 0.49 | 0.23 | 0.045 | 1.5 | 12.1 | 0.017 | - | - |
| 9 | 650-750 | 43.3 | 39.9 | 0.49 | 0.22 | 0.045 | 1.4 | 10.6 | 0.015 | - | - |
| 10 | 750-850 | 41.8 | 37.3 | 0.49 | 0.19 | 0.040 | 1.4 | 9.5 | 0.014 | - | - |
| 11 | 850-950 | 41.4 | 38.6 | 0.47 | 0.21 | 0.045 | 1.4 | 8.5 | 0.012 | - | - |
| 12 | 1050-1150 | 41.0 | 39.2 | 0.47 | 0.21 | 0.045 | 1.4 | 7.8 | 0.011 | - | - |
| 13 | 1150-1250 | 40.6 | 41.3 | 0.46 | 0.20 | 0.040 | 1.4 | 7.1 | 0 | - | - |

1. ED = equivalent depth (cm) of water in that layer.
2. The van Genuchten parameters $\theta_s$, $\theta_r$, $\alpha$ and n resulting from model calibration.
3. $K_{sat}$ = Saturated hydraulic conductivity. Values for layers 1-6 were measured in the field, but layers 7-13 are extrapolated from a power function (Fig. 3.7).
4. R = fraction of total fine root biomass in a layer. Live roots (0-2 mm) were measured to 6 m. Below 6 m it was assumed that each successive layer had 10% less root biomass than the layer above it.
5. Exchangeable K/Ca extracted with Mehlich I (Helmke and Sparks 1996; mg K/Ca per g soil in that layer).

**Table 3.2b Parameter values and initial values for stocks**

| TF fraction (unitless)[6] | Initial forest floor mass (mg litter)[7] | $K_{decomp}$ ($day^{-1}$)[8] | Canopy leaching K (unitless)[9] | Canopy leaching Ca (unitless)[9] | K $K_d$ ($cm^3\ g^{-1}$)[10] | Ca $K_d$ ($cm^3\ g^{-1}$)[10] |
|---|---|---|---|---|---|---|
| 0.88 | 80 | 0.0023 | 0.90 | 0.60 | 75 | 50 |

6. TF fraction= portion of rainfall that becomes throughfall and reaches the soil.
7. Forest floor litter includes leaves, small twigs and reproductive parts (mg litter per $cm^2$ area).
8. $K_{decomp}$= decomposition rate for forest floor litter.
9. The fraction of K/Ca in throughfall contributed by canopy leaching; estimated from D. Markewitz (unpublished data).
10. $K_d$ = partition coefficient between solution and adsorbed phases of K or Ca.

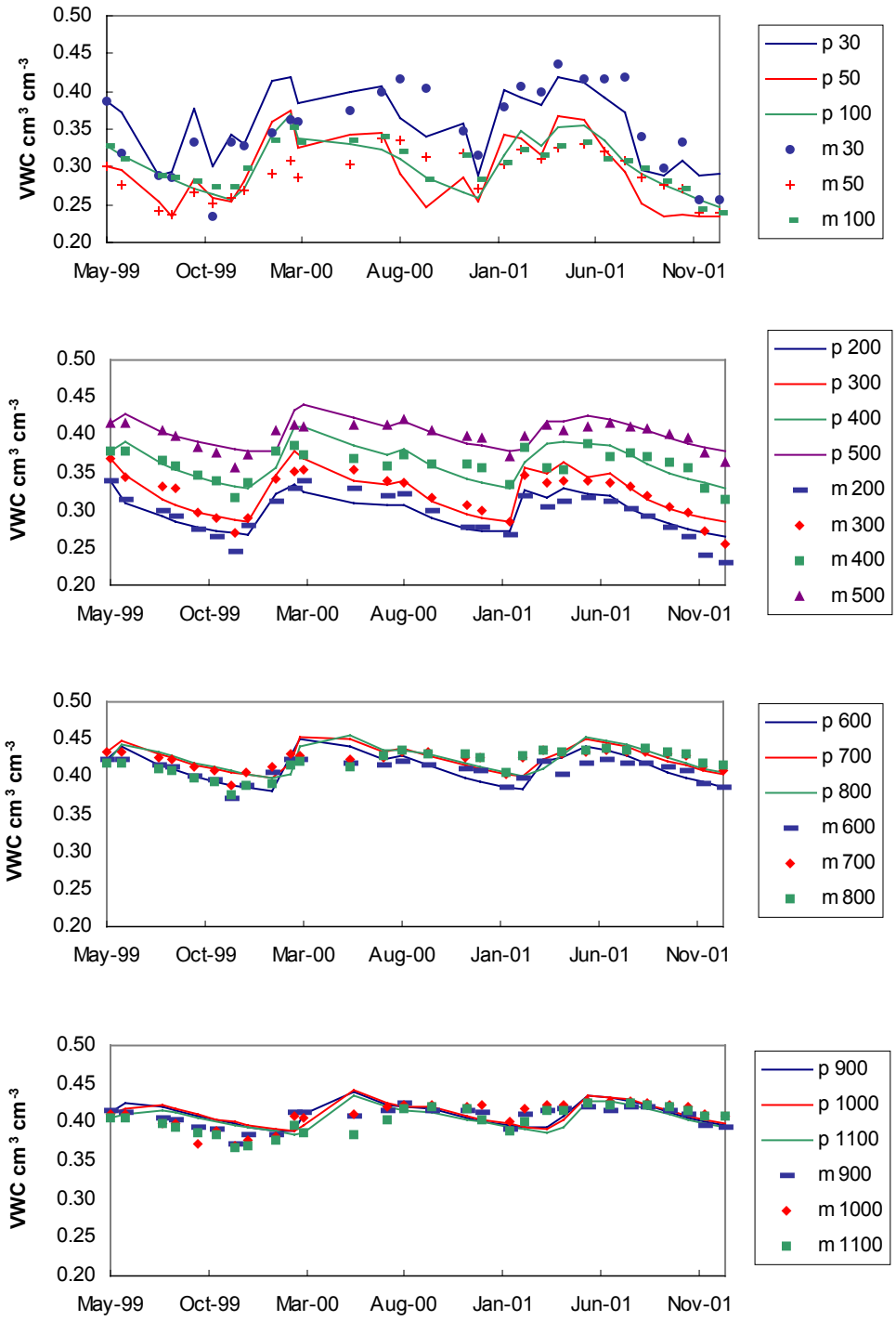


**Figure 3.9 Monthly measured (m) versus predicted (p) volumetric water contents (VWC) in the control plot, Tapajós National Forest, Brazil. Both series are labeled with the depth in cm. Measured VWCs are averages of 6 TDR sensors per depth.**

the model predictions may be about a month or two slower than the measured data. This probably reflects the limitations of using a darcian steady flux approach that does not allow water flux to vary with time and cannot account for a kinematic pressure wave response to perturbations such as rainfall infiltration or soil water extraction. Kinematic pressure waves typically propagate through unsaturated materials at much higher velocities than darcian approaches predict (Rasmussen et al. 2000). The model simulates a lag of one day or less between the top three horizons, and a lag of approximately 5-10 days for each additional meter. The time required for a wetting peak to arrive at the $11^{th}$ meter is on the lower end of that range, while the time for a depletion low to arrive at depth is on the higher end. The average delay is less than the 12-14 days $m^{-1}$ Jipp et al. (1998) inferred from TDR measurements for a *terra firme* forest near Paragominas, Pará.

The soil moisture characteristic (SMC) curves that result from the calibrated VG parameters are displaced below the curves fit to laboratory data so that the water content at each tension is lower (Figure 3.10). For comparison, SMC curves resulting from the average parameters for tropical soils with clay textures and for tropical soils in the Ferralsol FAO soil group reported by Hodnett and Tomasella (2002) are included. Taking the difference between the water content at 30 kPa and the water content at 1500 kPa to represent the maximum plant-available water (PAW), all of the SMC curves have 6.2-6.9% available water. Not only do the laboratory data have the lowest average range of water contents between $\theta_s$ and $\theta_r$ (0.216 $cm^3$ $cm^{-3}$), the SMC curve is also the highest primarily due to a smaller average n value.

In all cases, the optimized $\theta_s$ values are lower than the porosities measured in the laboratory. The values of $\alpha$ are moderately high, which reflects the presence of pores that

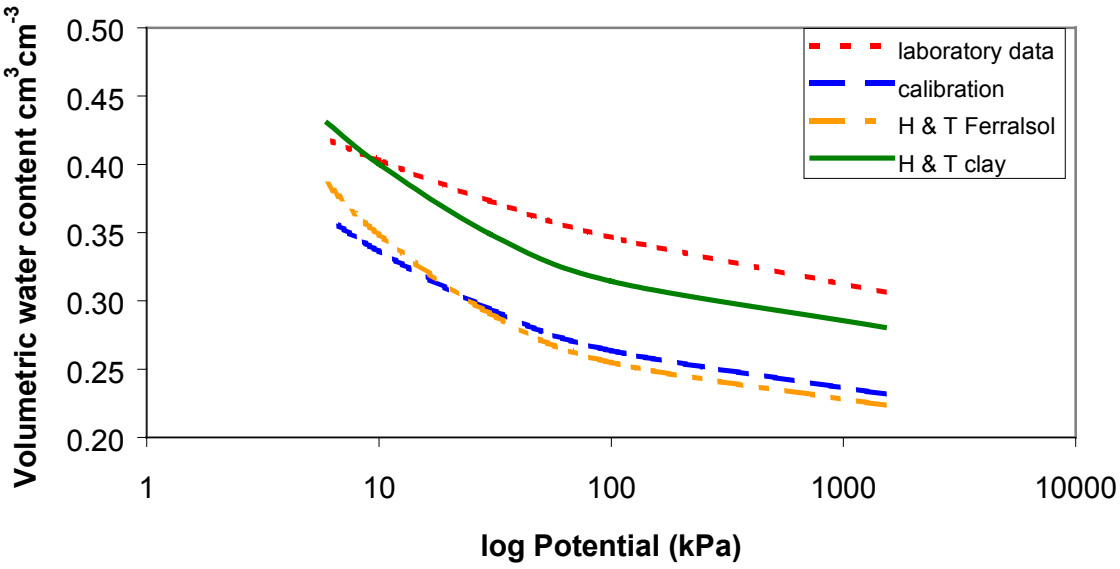


**Figure 3.10 Soil moisture characteristic curves described by the van Genuchten parameters fit to laboratory pressure plate data and by the parameters resulting from model calibration. For comparison, the curves described by the average parameters for tropical soils with clay textures and for tropical soils in the Ferralsol soil group as reported by Hodnett and Tomasella (2002) are shown.**

empty with small changes in potential. Kaolinite clays do not swell and have higher α because they drain from saturation quickly (Hodnett and Tomasella 2002). The SMC curve for the averages of the calibrated parameters closely resembles the average for tropical Ferralsols. The soil at the study site being modeled is classified as a Latosol in the Brazilian taxonomy, which is almost synonymous with the FAO concept of a Ferralsol. The most notable difference between the parameters is that the average range of water contents ($\theta_s$ - $\theta_r$) for the calibration parameters is much lower, 0.234 $cm^3$ $cm^{-3}$ compared to an average of 0.322 $cm^3$ $cm^{-3}$ for the Ferralsols.

***Results of Sensitivity Analysis***

Sensitivity analyses of four of the soil layers (layers 1, 4, 8 and 13) show that the model is sensitive to $\theta_s$, $\theta_r$, and n but not to α or $K_{sat}$ (Figure 3.11a). The results from the four layers were very similar. The sensitivity of the model to the VG parameters is not unexpected given that they are used in both the equation that determines matric potentials and the equation for unsaturated hydraulic conductivities. Even for the parameters to which the model is most sensitive, the effect of a change in one layer is largely confined to that layer. For example, raising the $\theta_s$ in a layer from 0.40 to 0.60 (40 to 60% water content) increased the average soil moisture of that layer by 10.6-13.6%, but the average water content of the layer above or below it generally decreased by 1% or less. The relative patterns in sensitivity remain the same for the average water content of the entire profile, but the increase is only 0.2-1.1% (Figure 3.11b). Changing $\theta_r$ in a layer from 0.10 to 0.30 (10 to 30% water content) increased the average soil moisture of the layer by 3.8-8.5%. In contrast, a 100-fold increase in $K_{sat}$ resulted in only a 1-2% decrease in the

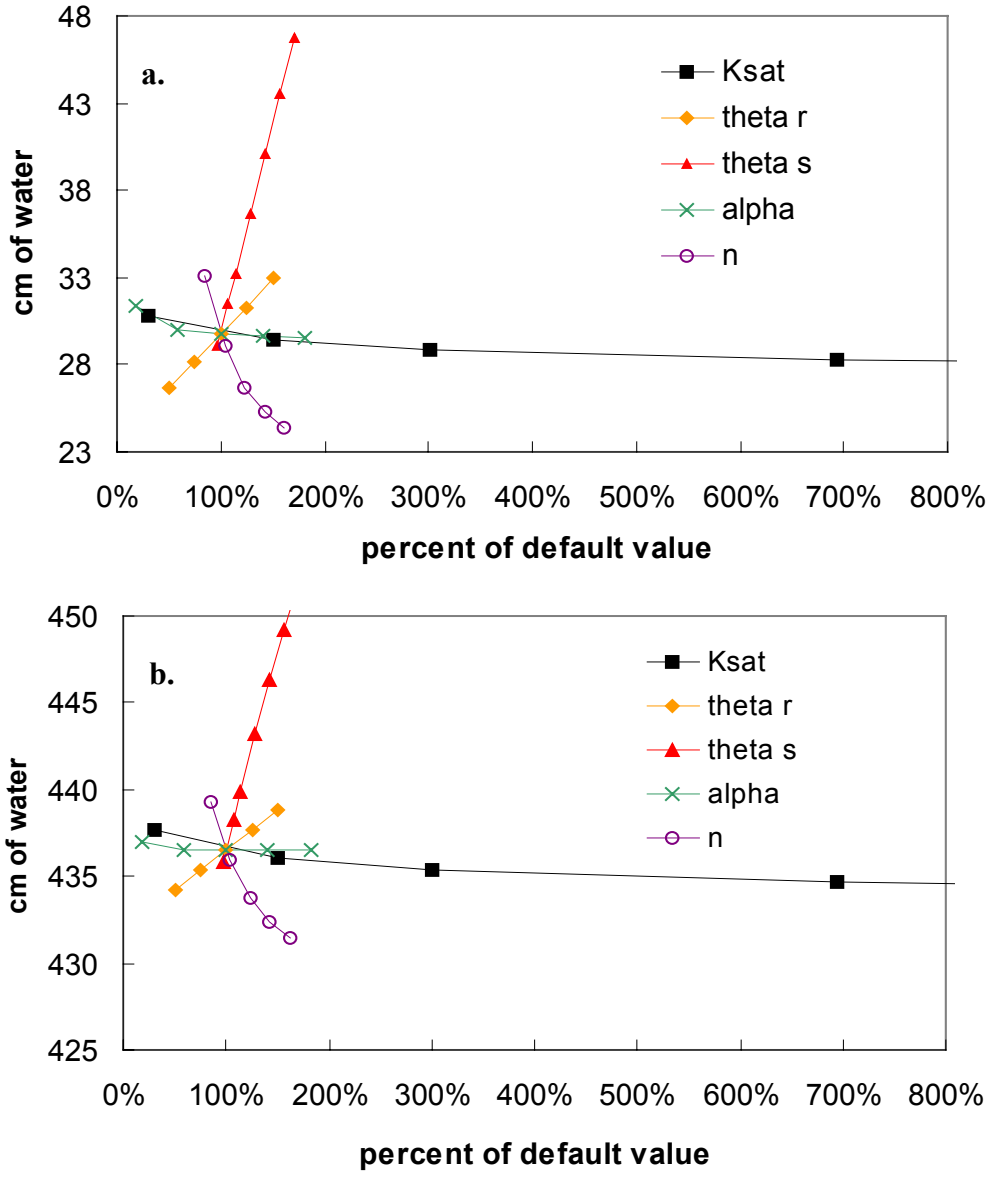


**Figure 3.11 a.) Sensitivity analysis of $\theta_s$, $\theta_r$, $\alpha$, n and $K_{sat}$ for 150-250 cm showing the effect of a change in the parameter values on the average depth of water in that layer over the 960 day simulation period. b.) Sensitivity analysis of $\theta_s$, $\theta_r$, $\alpha$, n and $K_{sat}$ for 150-250 cm showing the effect of a change in the parameter values on the average depth of water in the entire 11.5 m profile over the 960 day simulation period. The percent change in parameter values is relative to the default values listed in Table 3.2.**

water content of a layer. The water content is somewhat sensitive to $K_{sat}$ when the value is low. This is because $K_{sat}$ represents the maximum flow rate, so if its value for a layer is below the rate of water input from rain or drainage, the water content of the soil will increase. Once $K_{sat}$ is above the usual rate of water input, additional increases in the value have little effect.

In the above analyses, the sensitivity of the model to changes in individual VG parameters was tested. However, the four parameters work together to define the water retention and unsaturated flow rates. A full factorial analysis of the interaction between $\theta_s$, $\theta_r$, and n for the 150-250 cm layer confirms that the model is also sensitive to the difference between $\theta_s$ and $\theta_r$. This difference is more important than absolute values because it indicates the range of water contents expected in the soil (and the range for which the van Genuchten and Mualem models are valid). The difference between the average water content of the layer when $\theta_s$ is high (0.6 $cm^3$ $cm^{-3}$) and $\theta_r$ is low (0.1 $cm^3$ $cm^{-3}$) versus when $\theta_s$ is low (0.4 $cm^3$ $cm^{-3}$) and $\theta_r$ is high (0.3 $cm^3$ $cm^{-3}$) is about 2%, but when both parameters are low or high the difference in water content was 19.5%.

It is not uncommon for $K_{sat}$ to vary by orders of magnitude depending on the method used to measure it. To see how significant a methodological bias in the $K_{sat}$ estimates as a whole might be, five model runs were completed in which all $K_{sat}$ values were changed from their original values as follows:

1. No change
2. Adding 100 cm $day^{-1}$ to the $K_{sat}$ rate for each layer
3. Adding 10 cm $day^{-1}$ to each $K_{sat}$ rate
4. Doubling the rates
5. Halving all of the rates

Changing $K_{sat}$ did not affect the plant uptake significantly, but the average depth of water in the 11.5 m profile decreased by almost 48 cm (4.3% water content) when 100 cm $day^{-1}$ was added to each rate (Figure 3.12). Note that the new $K_{sat}$ in the top layer was 1.4 times greater than its original value and 15 times the original value in the bottom layer. The water content declines with increasing $K_{sat}$ because a higher rate allows water to drain out of the profile faster. However, adding 10 cm $day^{-1}$ or doubling each rate only changed the total depth of water by 14 cm over the 11.5 m (1.3% water content). Halving the rates added 15 cm to the average depth of water (1.4% water content). Though $K_{sat}$ is a highly variable soil property, the effect on soil water in the model is not dramatic.

The PET rate directly affects the amount of plant uptake, indirectly influencing soil moisture. A doubling of daily PET rates increases cumulative plant uptake to 504 cm, or 70% greater than the previous prediction, and decreased the average total depth of water in the profile to 395 cm, a 10% decrease. Halving the PET resulted in a halving of the cumulative plant uptake to 147.6 cm but only a slight increase of 15 cm in the average total depth of water in the profile.

A higher throughfall fraction means that a lower portion of rainfall is intercepted and there is more throughfall to enter the soil. However, changing the fraction did not seem to have an effect on the average depth of water in the soil profile because plant uptake compensated for the difference (Figure 3.13). For example, changing the fraction from 0.88 to 0.93 added 25 cm of water to the soil over the simulation period, but plant uptake increased by 26 cm. Changing the fraction from 0.88 to 0.8 meant that 40.5 cm less water reached the soil, but plant uptake decreased by 41.5 cm.

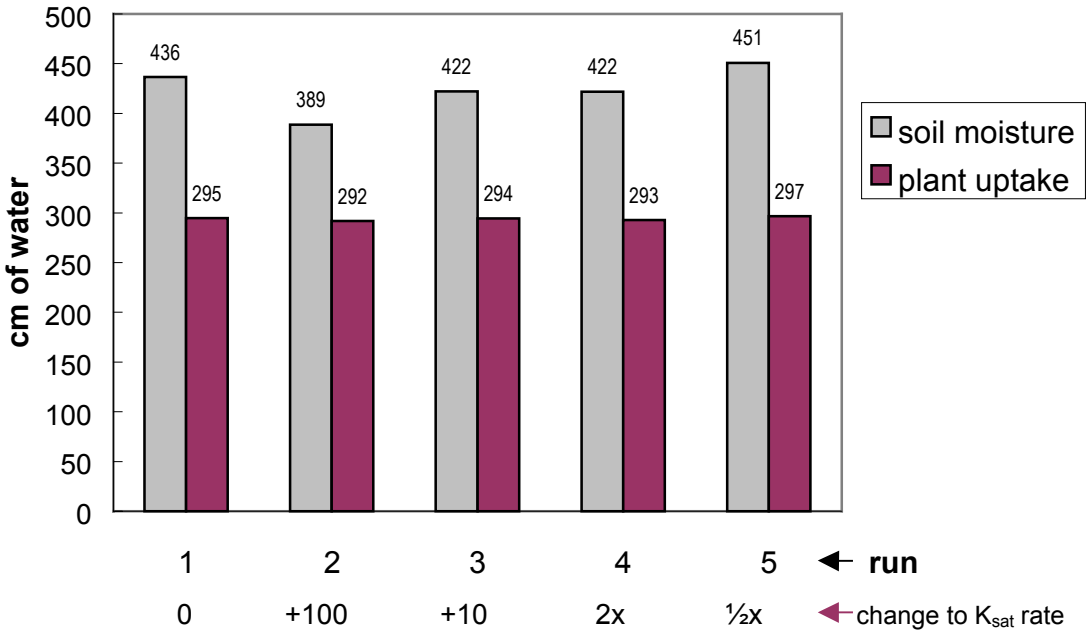


**Figure 3.12 Effect of different $K_{sat}$ values on the average depth of water in the 11.5 m profile and on the cumulative plant uptake over the 960 day simulation period. For each run, $K_{sat}$ values were changed from the default values listed in Table 3.2a as follows: 1. No change 2. Adding 100 cm $day^{-1}$ to the rate for each layer 3. Adding 10 cm $day^{-1}$ to the rate for each layer 4. Doubling each rate 5. Halving each rate.**

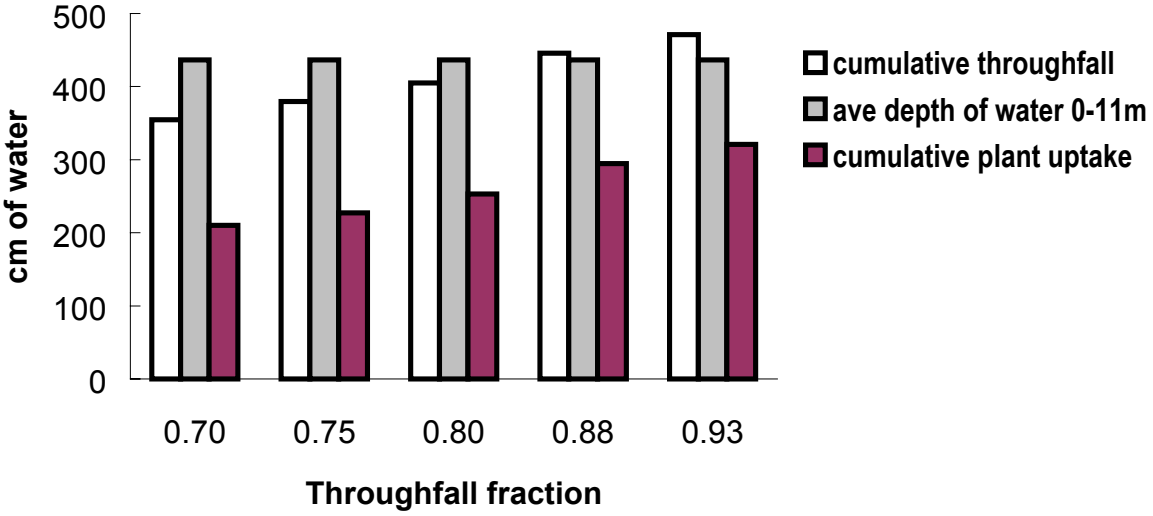


**Figure 3.13 Effect of varying the throughfall fraction from a default value of 0.88 on the average depth of water in the 11.5 m profile and on cumulative plant uptake over the 960 day simulation period.**

Sensitivity analysis for the nutrient component of the model examined the effect of uncertainty in the litter decomposition rate coefficient and the partition coefficients. The results from varying the litter decomposition rate coefficient were as expected. Further increases in the rate did not increase the introduction of K or Ca to the soil as much as decreasing it reduced the introduction (Figure 3.14). The change in Ca is greater than K because the concentration of Ca in litter is higher.

In theory, a partition coefficient ($K_d$) represents the ratio of solid to liquid concentrations at which the two phases are in equilibrium and no exchange occurs. Decreasing a $K_d$ increases desorption from particle surfaces to solution, resulting in more leaching of that element and vice versa. Lowering the $K_d$ for K to 25% of its original value of 75 $cm^3\ g^{-1}$ increased leaching by 10 times and the average solution concentration by 3% but increasing the value had much less of an effect (Figure 3.15a). Decreasing the $K_d$ for Ca to 20% of its original value of 50 $cm^3\ g^{-1}$ increased leaching by more than 200 times, while the average concentration of Ca in solution increased 2.7 times. As with K, further increases in the Ca partition coefficient were not as dramatic (Figure 3.15b).

***Predictions of water content in the treatment plot***

The 89.5 and 81.7 cm of throughfall the model excludes from the treatment plot for the 2000 and 2001 rainy seasons is slightly greater than the 89 and 68 cm estimated through field observation by the researchers of the exclusion experiment (D. Nepstad unpublished data). The RMSE between predicted and measured soil moisture is 3.1% water content (the average standard errors of six measurements are 1-2% water content). This is a RRMSE of 9.2%. The mean difference is -0.65±-0.16% water content.

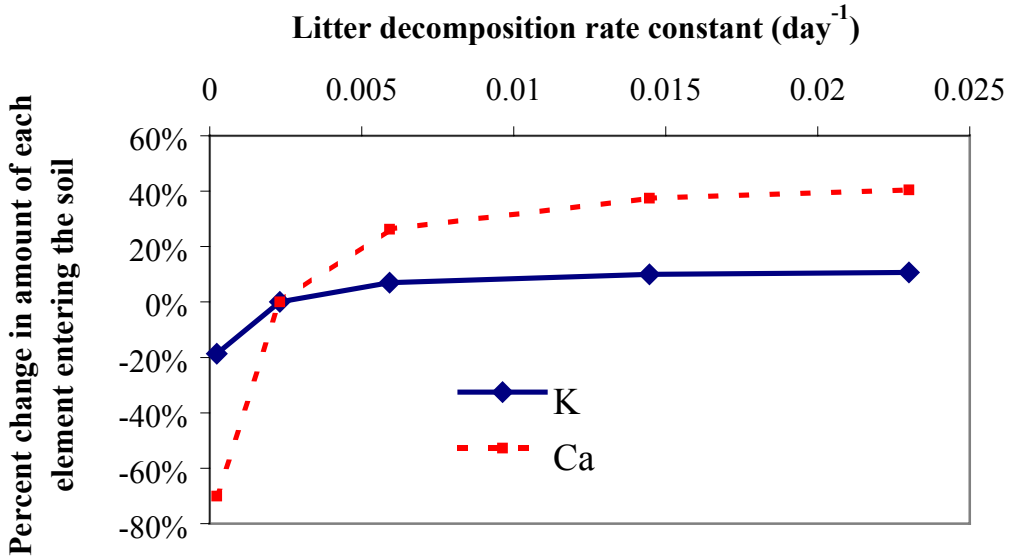


**Figure 3.14 Effect of changing the litter decomposition rate from 0.0023 day$^{-1}$ on the amount of K and Ca entering the soil.**

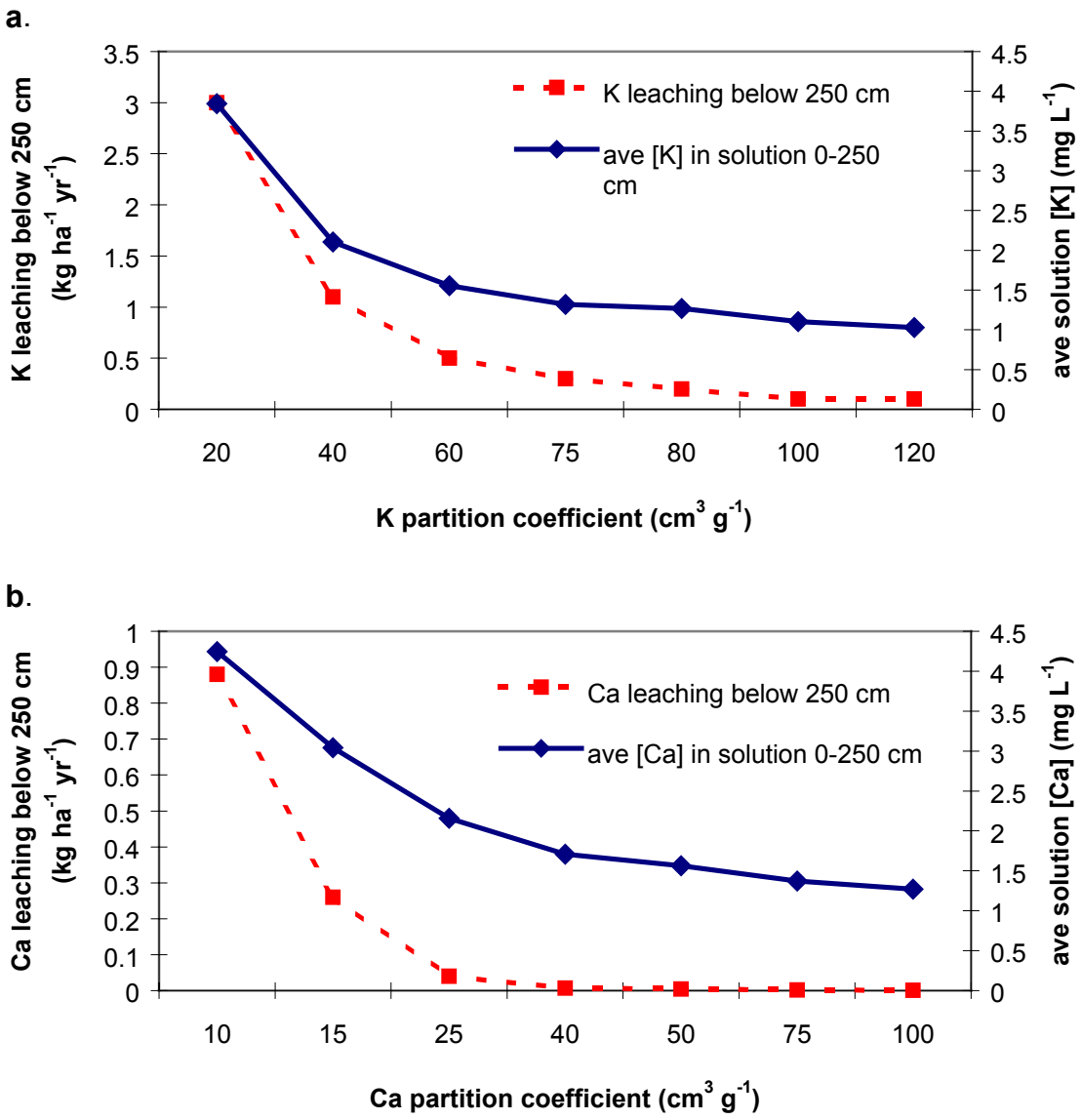


**Figure 3.15 Sensitivity analysis of partition coefficients ($K_d=C_s/C_l$) for a.) potassium and b.) calcium showing the effect on the amount of each element leaching below 250 cm depth and on the average concentration of the elements in solution.**

Overall the model was able to explain about 73% of the variability in the volumetric water content data (Figure 3.16). The model over-predicts lower TDR readings and slightly under-predicts the wetter ones. However, it is important to remember that there is measurement error associated with the TDR data. TDR sensors have been shown to be most sensitive to conditions immediately surrounding the rods (Baker and Lascano 1989; Knight 1992). If the installation of a sensor is poor and/or the soil pulls away slightly upon drying, then air will contact the rods and the measured soil moisture will be less than the actual (Knight et al. 1994). In fact, in early 2000, many TDR probes were replaced at the research site due to suspected poor functioning. If it is true that the TDR probes were underestimating water contents during the first eight months of the experiment, the model prediction error would be lower.

The timing of the model predictions for depletion and wetting below 1 m seems to be offset by 1-3 months later (Figure 3.17). From 6-11 meters the model simulates a greater draw-down of water than the TDR data indicate, especially during the second post-treatment rainy season. This disagreement could be due to incorrect assumptions regarding the root distribution or $K_{sat}$ in those layers. Specifically, there may be fewer roots and/or the roots are not as active as assumed, leading to less plant uptake from those depths, and/or the $K_{sat}$ values may be too high, draining the layers too fast.

***Rainfall Partitioning***

Over the 960-day simulation period, there was an average of 0.527 cm $day^{-1}$ rainfall, 0.464 cm $day^{-1}$ throughfall, and 0.063 cm $day^{-1}$ interception. On an annual basis, the 192.5 cm of rainfall is near the average of 200 cm reported by Nepstad et al. (2002)

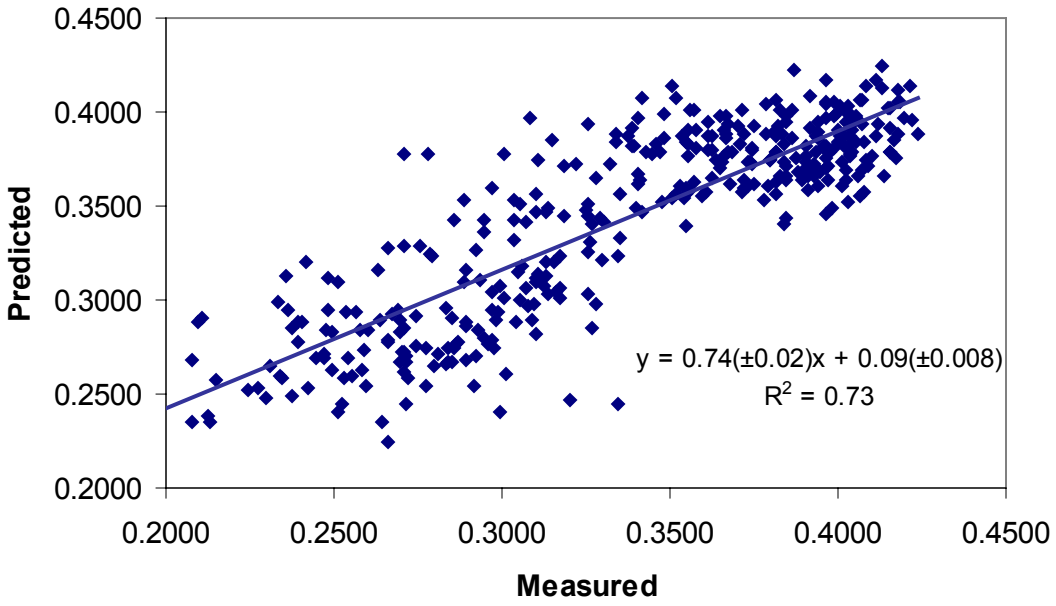


**Figure 3.16 Correlation between measured and predicted volumetric water contents (VWC) in the treatment plot, Tapajós National Forest, Brazil. The comparison is for 29 dates between May 1999 and December 2001 on which VWC was measured at the field site.**

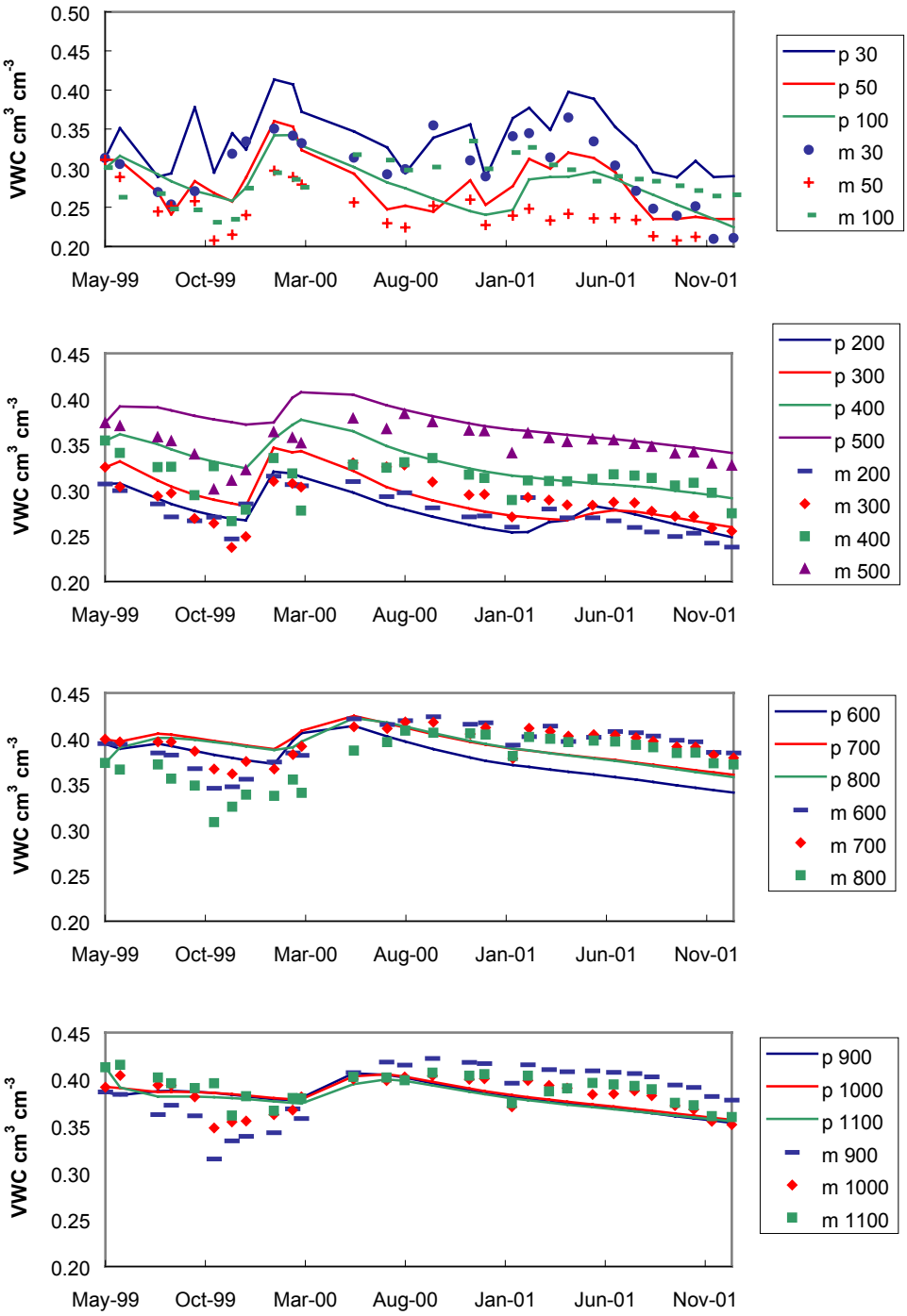


**Figure 3.17 Monthly measured (m) versus predicted (p) volumetric water contents (VWC) in the treatment plot, Tapajós National Forest, Brazil. Both series are labeled with the depth in cm. Measured VWCs are averages of 6 TDR sensors per depth.**

for this site. The average belies the fact that in 2000 the rainfall was about 24% above normal (246.9 cm) and in 2001 rainfall was 10% below normal (179.8 cm). In the model, the throughfall fraction is always 88% of gross rainfall. The use of a set fraction does not consider variability for different storm characteristics or time periods. Nepstad et al. (2002) reported 20% interception at this site from February to July 2000. The average throughfall fraction used in the model is only slightly higher than the average 82-87% measured by Marin et al. (2000) for a forest in the Columbian Amazon and the 86-87% estimated by Ubarana (1996) for two *terra firme* forest sites near Marabá and Ji-Paraná in Brazil.

***Evapotranspiration***

In the control plot simulation the average evaporation of 0.063 cm $day^{-1}$ intercepted rainfall plus the average transpiration of 0.307 cm $day^{-1}$ plant uptake yields an actual evapotranspiration (AET) rate of 0.37 cm $day^{-1}$. Water balance studies have calculated ET rates of 0.415 cm $day^{-1}$ for an eastern Amazonian forest (Jipp et al. 1998) and 0.41 cm $day^{-1}$ for the central Amazon (Leopoldo et al. 1995). The simulated AET in the control plot is below these estimates, but is very similar to the 0.359 cm $day^{-1}$ reported by Shuttleworth (1988) and to the 0.365 cm $day^{-1}$ average for 2 years of field eddy correlation measurements near Manaus (Rocha et al. 1996). In fact, the average control plot AET rate equals the value Klinge et al. (2001) simulated for an eastern Amazonian forest from a model using the Penman equation for PET and a matric-potential dependent reduction function.

PET is typically highest in the dry season due to a higher vapor pressure gradient between air and leaf surfaces. The model predicts that AET is equal to PET for most of the year, except during the dry season when soil moisture becomes limiting (Figure 3.18). On average, AET was 80% of PET, which was calculated to be about 0.46 cm $day^{-1}$ using the modified Thornthwaite model. Villa Nova et al. (1976) found the same relation between AET and PET, but estimates as high as 98% have been reported (Ribeiro and Villa Nova 1979). Transpiration (uptake) is 83% of AET, which is the same percentage Leopoldo (1995) reported, even though his estimates of AET were higher.

In the treatment simulation, AET declined by 0.0125 cm $day^{-1}$. Because of the model structure, all of the decrease occurred in plant uptake (i.e. transpiration). Considering the exclusion of throughfall by the panels, only 0.285 cm $day^{-1}$ water reached the soil in the treatment plot, as opposed to 0.464 cm $day^{-1}$ in the control plot. Although less water is returned to the atmosphere in the treatment plot simulation, the AET is 25% higher than the inputs that arrived at the soil. However, as discussed above, the simulated water contents below 6 m were consistently lower than the measured values during the second treatment year (Figure 3.17), and it is likely that the input and AET rates would be more similar if those predictions were higher. While evapotranspiration may exceed inputs for brief periods of time, if this were to continue, the water storage in the soil would become depleted.

Excepting the top two layers, where uptake is restricted during the dry season, the fraction of actual uptake coming from each layer in the control plot strongly follows the assumed root distribution. The same is true for the treatment plot, although the uptake

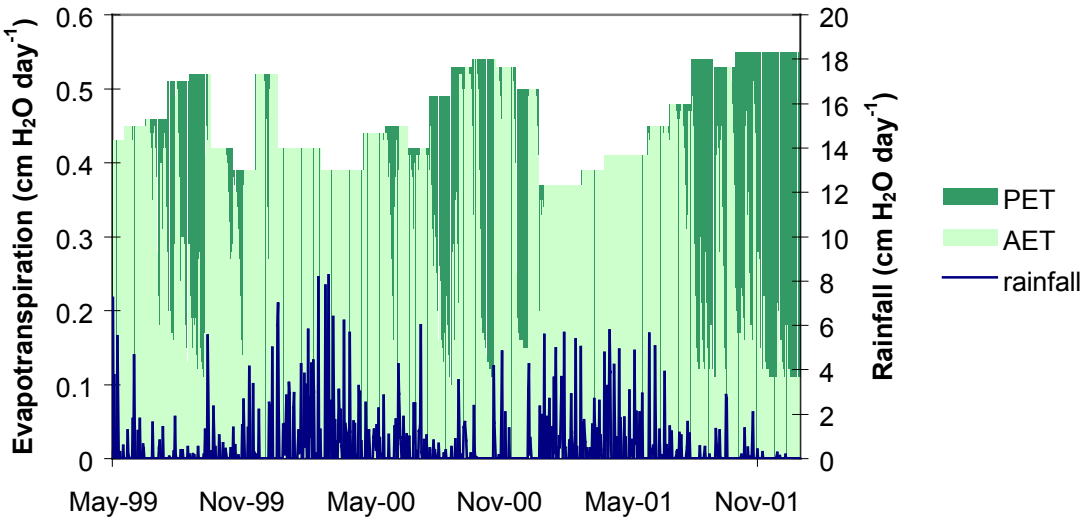


**Figure 3.18 Potential evapotranspiration (PET) and simulated actual evapotranspiration (AET) for the Tapajós National Forest, Brazil. The dark green areas represent periods of water deficit when AET is less than PET.**

from the top two layers is more restricted. The layers at 1 meter and below became slightly more important contributors to uptake as the exclusion treatment continued.

***Water movement and storage***

The $K_{sat}$ values vary from 273 cm $day^{-1}$ in the first layer to 7.1 cm $day^{-1}$ in the last layer (Figure 3.8). These values are within the 1.7-552 cm $day^{-1}$ range measured by researchers at another *terra firme* forest site in Paragominas with similar, deeply weathered Oxisols (A. Schuler unpublished data). The $K_{sat}$ rates correspond to $10^{-5}$ to $10^{-7}$ m $s^{-1}$, which is fast for clay and more similar to rates expected in coarser textured soils (Hillel 1998).

Not surprisingly, the unsaturated hydraulic conductivity ($K_{unsat}$) rates are markedly reduced from the maximum rates achieved at saturation. The simulated $K_{unsat}$s for the control plot are on the order of $10^{-7}$ m $s^{-1}$ at the surface to $10^{-9}$ m $s^{-1}$ at other depths, while in the treatment plot the simulated $K_{unsat}$s are on the order of $10^{-8}$ m $s^{-1}$ at the surface to $10^{-9}$ m $s^{-1}$ at other depths. The lower rates in the treatment plot mean that less water drains past each layer than in the control where the water fluxes are 3-4 times greater (Table 3.3). Before the treatment was applied, similar amounts of water drained through the profiles in both plots. After the panels were first installed in early February 2000, the average control plot fluxes went up due to the arrival of more rain. But in the treatment plot, the average fluxes decreased at that time. The fraction of water lost to deep drainage is smaller under the treatment. In the control plot, about 45% of water input to the soil is drained past 1150 cm, compared to 17% in the treatment plot. The slower rates of water flow and lower steady water fluxes in the treatment plot are due to

**Table 3.3 Simulated average annual fluxes of water in the control and treatment plots, Tapajós National Forest, Brazil, May 1999 to Dec 2001. The change in water storage is given for the soil profile from 0-1150 cm.**

| | Control | Treatment |
|---|---|---|
| | ----- cm year$^{-1}$----- | |
| Rainfall | 193 | 193 |
| Interception | 23 | 23 |
| Exclusion | 0 | 66 |
| Throughfall | 169 | 104 |
| Evapotranspiration | 135 | 130 |
| Flux past soil depth: | | |
| 40 cm | 102 | 38 |
| 75 cm | 90 | 28 |
| 150 cm | 86 | 23 |
| 250 cm | 84 | 21 |
| 350 cm | 84 | 20 |
| 450 cm | 83 | 20 |
| 550 cm | 82 | 19 |
| 650 cm | 81 | 18 |
| 750 cm | 80 | 18 |
| 850 cm | 79 | 16 |
| 950 cm | 78 | 16 |
| 1050 cm | 77 | 16 |
| 1150 cm | 77 | 18 |
| Δ Water storage | -20 | -21 |

the lower water contents (more negative potentials) of the layers. It is important to note that the 2.5 year time span for which the simulated fluxes of Table 3.3 are reported covers both pre- and post-treatment periods and includes three dry seasons but only two wet seasons. During the 2-year period from May 1999 to May 2001, net inputs (rain – evapotranspiration = 83.2 cm $year^{-1}$) were higher than drainage (75.86 cm $year^{-1}$) in the control plot. However, the water deficit that developed during the seven months between May 2001 and December 2001 (rain – evapotranspiration = -44.5 cm) was strong enough to result in an average net loss from water storage of 20 cm $year^{-1}$ for the entire simulation period.

The measured water contents in the control plot show that the soils at depth are wetter than near the surface (Figure 3.19a). During the dry season, water from the entire profile is drawn down, especially in the upper profile where there is a higher concentration of roots. By the middle of the rainy season, the surface soils rewet and the water storage below four meters recharges. The soils in the treatment plot were drier than the soils in the control plot even before the exclusion panels were first installed in February 2000 (Figure 3.19b). Because the dry season preceding the first treatment period and the treatment period itself were wetter than average, the panels did not divert enough water to invoke drought stress in the vegetation within the treatment plot (Nepstad et al. 2002). However, during the second treatment period, the soil near the surface dried out more extensively and the recharge at depth was not complete. The predicted water contents show similar patterns with depth, the most notable difference being that the current model predicts that the soil below 500 cm in the treatment plot dries out more than measured during the second treatment year (Figure 3.20).

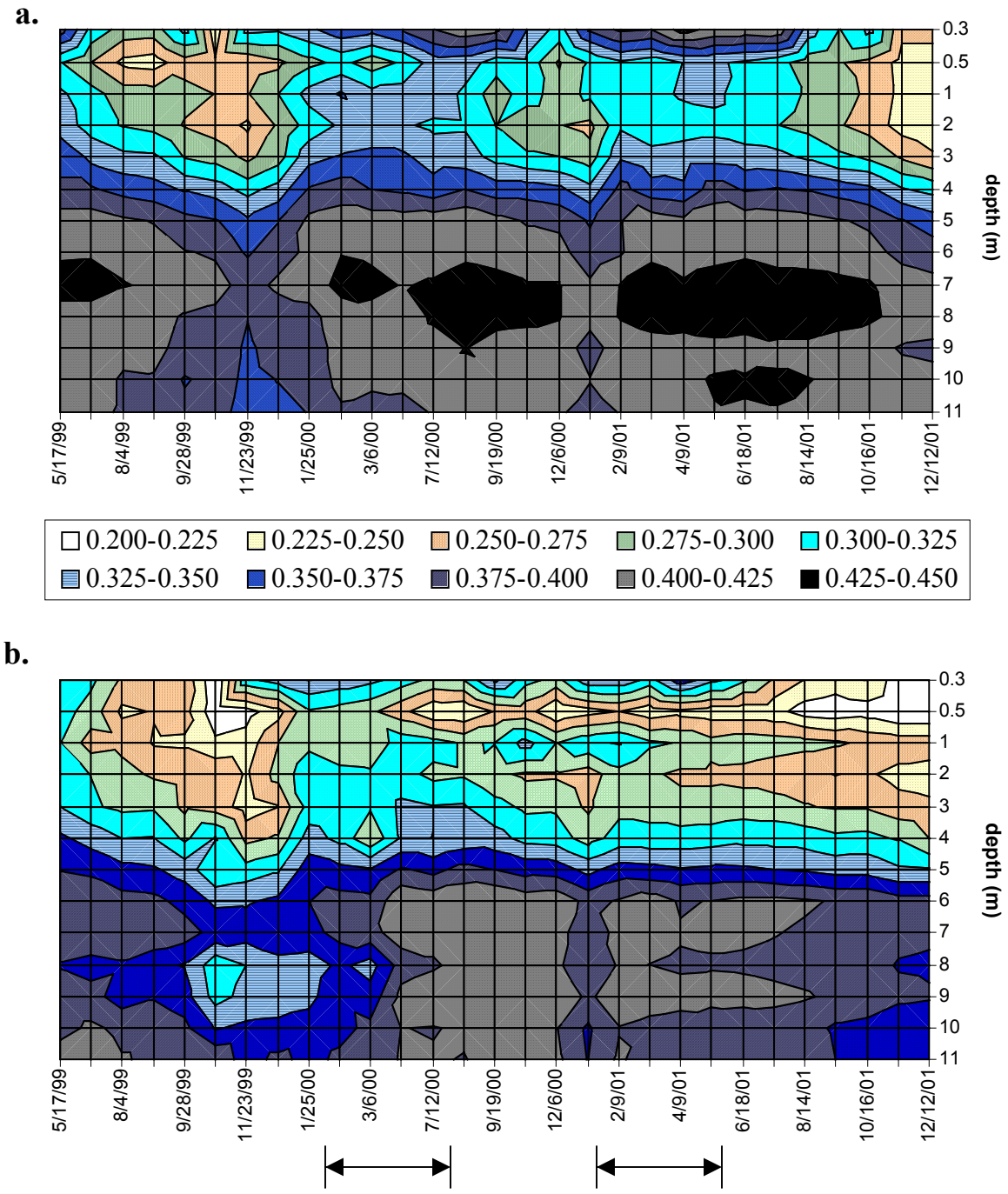


**Figure 3.19 Measured water contents ($cm^3\ cm^{-3}$) in the a.) control plot and b.) treatment plot, Tapajós National Forest, Brazil. Each depth is an average of 6 sensors. Periods of throughfall reduction in the treatment plot are indicated by arrows.**

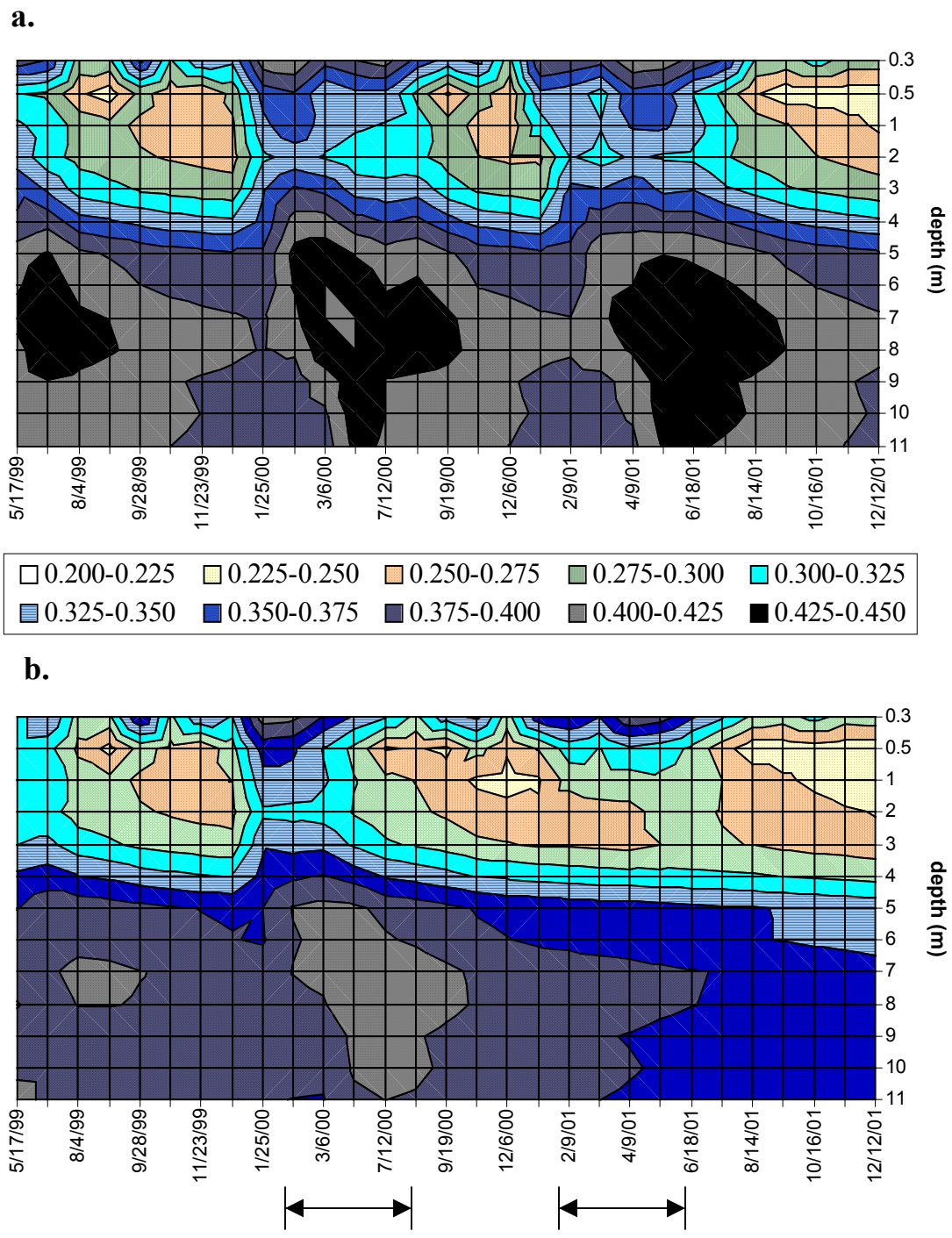


**Figure 3.20 Simulated water contents ($cm^3\ cm^{-3}$) in the a.) control plot and b.) treatment plot, Tapajós National Forest, Brazil. Periods of throughfall reduction in the treatment plot are indicated by arrows.**

***Nutrient fluxes***

The hydrologic cycle constrains biogeochemical cycling to such an extent that it is not possible to construct nutrient budgets without appropriate knowledge of the fluxes of water into and out of the system under study (Likens and Bormann 1995). In the current experiment, there is particular interest in assessing whether decreasing solution fluxes would increase concentrations (due to a lower dilution effect) such that element fluxes would remain consistent, or whether the diminished water fluxes associated with drought would alter nutrient fluxes by impacting other forest functions (eg. root death). Table 3.4a lists the predicted nutrient fluxes for both the control and treatment plots of the study site. For comparison, the results from a study of nutrient cycling in a *terra firme* forest in Paragominas, Pará are provided (Markewitz et al. in press). The model predicts higher inputs of K and Ca to the soil, even for the treatment plot where the average annual throughfall of 104 cm is about equal to the 103 cm measured during the Paragominas study. In the control plot, the much higher annual throughfall of 169 cm could partly account for some of the additional inputs.

Markewitz et al. (in press) assume that plant uptake of nutrients can be predicted by the amount needed to replace nutrients lost in fine litterfall and canopy leaching, since the mature forest is neither aggrading or degrading in the long-term. This is the same approach used in the current model. The difference between plant uptake of nutrients and the flux of nutrients into the soil is due to contributions from rainfall and any errors in our estimates of elements in daily throughfall or canopy leaching. Daily throughfall nutrient fluxes are predicted by functions that explain only 46 and 30% of the variability in K and Ca, respectively (Figure 3.7), while canopy leaching is simulated based on a fixed ratio.

**Table 3.4a Simulated fluxes of K and Ca in the control and treatment plots, Tapajós National Forest, Brazil, May 1999 to Dec. 2001. Fluxes from Markewitz et al. (in press) are also provided.**

| | Potassium (kg/ha/yr) | | | Calcium (kg/ha/yr) | | |
|---|---|---|---|---|---|---|
| | Control | Treatment | Markewitz | Control | Treatment | Markewitz |
| Rainfall | 6.9 | | 5 | 7 | | 3 |
| Throughfall | 69 | 61 | | 17 | 13 | |
| Litter decomposition | 24 | 24 | | 120 | 120 | |
| Flux into the soil | 93 | 85 | 65 | 136 | 134 | 115 |
| Plant uptake | 87 | 79 | 65 | 134 | 132 | 115 |
| Flux past soil depth: | | | | | | |
| 40 cm | 9.1 | 3.5 | 1.4[a] | 9.1 | 3.8 | 9.9[a] |
| 75 cm | 1.9 | 0.3 | | 1.7 | 0.3 | |
| 150 cm | 0.6 | 0.1 | | 0.2 | 0.02 | |
| 250 cm | 0.3 | 0.1 | | 0.004 | 0.00006 | |

[a] Flux past 25 cm.

**Table 3.4b Predicted solution concentrations in the control (C) and treatment (T) plots, Tapajós National Forest, Brazil, May 1999 to Dec. 2001. Measured concentrations are for solutions collected between May 1999 and Aug. 2001 from lysimeters buried under the forest floor or installed at 25 cm and 200 cm depths (n=3 per plot).**

| | Potassium (mg/L) | | | | Calcium (mg/L) | | | |
|---|---|---|---|---|---|---|---|---|
| | Predicted | | Measured | | Predicted | | Measured | |
| | C | T | C | T | C | T | C | T |
| Litter leachate | | | 1.56[b] | 3.01[b] | | | 2.18[b] | 2.27[b] |
| 0-40 cm | 1.04 | 1.12 | 0.21[c] | 0.36[c] | 1.63 | 1.77 | 1.12[c] | 3.06[c] |
| 40-75 cm | 0.08 | 0.02 | | | 0.08 | 0.02 | | |
| 75-150 cm | 0.06 | 0.04 | | | 0.008 | 0.001 | | |
| 150-250 cm | 0.05 | 0.05 | 0.15[d] | 0.40[d] | 0.0002 | 0.000005 | 0.92[d] | 1.03[d] |

[b] Average volume-weighted concentration for three zero tension lysimeters under the forest floor
[c] Average volume-weighted concentration for three tension lysimeters at 25 cm
[d] Average volume-weighted concentration for three tension lysimeters at 200 cm

The model predicts that more than six times as much K flows past the 0-40 cm soil layer in the control plot, but only slightly more Ca, than Markewitz et al. (in press) reported flowing past 25 cm lysimeters.

The reduction of throughfall in the treatment plot means that fewer nutrients are returned to the soil compared to the control plot (Table 3.4a). Despite the lower inputs to the soil under treatment, nutrient concentrations in the top layer are elevated (Table 3.4b), presumably due to a lower volume of water in which to dilute the nutrients present. Fewer nutrients are predicted to be lost to deep drainage in the treatment plot, however, as a result of the lower water fluxes.

Direct comparison of the predicted concentrations in the 0-40 cm layer with the measured concentrations for solutions collected by 25 cm-deep lysimeters is complicated because litter leachate is implicitly included in the top layer in the model (Table 3.4b). Considering this lumping of the layers, the predicted concentrations from 0-40 cm may be a reasonable average of the measured litter and 25 cm soil solution concentrations. The model simulated a more abrupt decrease in nutrient concentrations with depth than the measured data would indicate. If the moist tropical forests of the study site are in a steady state in relation to nutrient inputs and outputs, then rainfall inputs are high in comparison to model predictions of fluxes past 250 cm.

Unfortunately, the model behavior regarding cation exchange between soil and solution phases does not appear realistic. In the control plot, both K and Ca are continually adsorbed onto the soil from the solution in the first layer and are continually, though slowly, desorbed back to solution in the 3$^{rd}$ and 4$^{th}$ layers. In the treatment plot, both elements are continually adsorbed on to the soil from the solution in the top layer

and gradually desorbed in the others. Additionally, we did not have information on the partition coefficients ($K_d$s) for this site, so predicted values from the literature were used. Partition coefficients are affected by soil properties such as texture, structure, pH, and organic matter, as well as the concentration of pore water and the presence of competing cations. Because of these variables, values borrowed from the literature may lead to large errors in absolute amounts of cation movement (Sheppard and Thibault 1990). The sensitivity analysis showed that the solution concentrations were very sensitive to the use of lower values (Figure 3.15).

Nutrient fluxes estimated by multiplying the measured solution concentrations by the simulated water fluxes past 40 cm are 2.14 kg-K $ha^{-1}$ $year^{-1}$ and 11.42 kg-Ca $ha^{-1}$ $yr^{-1}$. These fluxes are on the order of the estimates reported by Markewitz et al. (in press) for Paragominas (Table 3.4a). The simulated flux of water past 40 cm is 2.7 times lower in the treatment than in the control plot (Table 3.3). The volume-weighted mean concentrations of Ca between 0-40 cm increased by a factor of 2.7, but K concentrations only increased by a factor of 1.7. Water fluxes past 250 cm were 4 times lower in the treatment than in the control, but the elevation of solution concentrations of K (2.7 times) and Ca (1.1 times) in the treatment plot were not as high. If only changes in soil moisture are responsible these changes in the solution concentrations, then nutrient fluxes and solution concentrations would be expected to respond in inverse but proportional ratios. These estimates suggest that other processes (e.g. adsorption) may be involved.

## Conclusions and Directions for Further Research

The darcian method for evaluating unsaturated steady water fluxes predicts measured soil volumetric water contents within 3% water content for the first 960 days of the throughfall exclusion experiment. As the experiment continues and the vegetation suffers more stress, simplifying assumptions of the model may limit its ability to fully capture the responses. One example is the use of a fixed root distribution. The model would benefit from a dynamic root distribution that accounts for growth and death in each layer and that considers root functionality. This would affect the simulated distribution of water and nutrient uptake between layers and would allow for the reintroduction of nutrients to the soil as roots die. Greater root growth at depth is hypothesized during the continued throughfall exclusion (Nepstad et al. 2002).

Other root functions may also affect soil moisture predictions. For example, if roots serve as passive conduits for redistributing water from wetter to drier regions of the soil, the soil water contents may not be predicted well unless this water movement is accounted for directly. Researchers associated with the throughfall exclusion experiment are currently testing whether such hydraulic lift occurs at this site.

To realistically model adsorption and desorption of cations, the equilibrium partitioning between particle surfaces and soil solution should be determined for this site. The current model does not appear to be predicting these exchanges well, which has a large effect on the simulated concentrations and therefore fluxes of nutrients. Competition by other cations for exchange sites may also be important.

Another suggestion for further model development would be to include the processes of leaf shedding and litter accumulation on the forest floor. As older leaves are

shed and new leaf production declines in response to drought stress, leaf area will decrease. Rainfall partitioning (i.e. the throughfall fraction) and nutrient inputs from both throughfall and litter decay should be related to these mechanisms. As the canopy opens and the sub-canopy climate changes, soil evaporation may also become more significant.

The model is very sensitive to the van Genuchten parameters, which are used to translate water contents to potentials and determine the functions for unsaturated water flow. Theoretically, the water retention properties these parameters describe are physical properties of the soil that can be quantified. If the laboratory-generated water retention data are correct, we should be measuring higher volumetric water contents in the field. However, the soil moisture characteristic curves resulting from model calibration are very similar to published curves for the same soil order. The curves also show similarly low plant-available water. Of course, neither measurement technique is free from error, so further research should be done to resolve this discrepancy. Because of stability issues in the model, it is advisable to minimize the effect of spatial heterogeneity by taking many samples at each depth and using the average values.

During the first treatment year, the measured water contents demonstrate and the model predicts mild soil water depletion near the surface. Persistence of the drought lead to more extensive drying of the surface soils and prevented complete recharge of water stored deeper in the soil. The model also predicts that evapotranspiration declines, and that water and nutrient fluxes are diminished in response to drought. The complex two-way interactions between vegetation and climate and the unique regional hydrology mean that frequent drought induced by global climate change and local land use conversion could be self-reinforcing.

**References**

Amorim, M. C. d., L. Rossato and J. Tomasella (1999). Determinação da evapotranspiração potential do Brasil aplicado o modelo de Thornthwaite a um sistema de informação geografica. Revista Brasileira de Recursos Hidricos 4(3): 83-90.

Baker, J. M. and R. J. Lascano (1989). The spatial sensitivity of time domain reflectometry. Soil Science 147(5): 378-383.

Barber, S. (1995). Soil Nutrient Bioavailability. John Wiley and Sons, New York. 414p.

Clesceri, L. S., A. E. Greenberg, and A. D. Eaton (eds). (1998). Standard Methods for the Examination of Water and Wastewater. United Book Press, Baltimore. 1325p.

Davidson, E. A. and S. E. Trumbore (1995). Gas diffusivity and production of $CO_2$ in deep soils of the eastern Amazon. Tellus 47B: 550-565.

Ehleringer, J. R. and T. E. Dawson (1992). Water uptake by plants: Perspective from stable isotope composition. Plant, Cell and Environment 15: 1073-1082.

Feddes, R. A., H. Hoff, M. Bruen, T. E. Dawson, P. de Rosnay, P. Dirmeyer, R. B. Jackson, P. Kabat, A. Kleidon, A. Lilly and A. J. Pitman (2001). Modeling root water uptake in hydrological and climate models. Bulletin of the American Meteorological Society 82(12): 2797-2809.

Feddes, R. A., P. J. Kowalik and H. Zaradny (1978). Simulation of Field Water Use and Crop Yield. Centre for Agricultural Publishing and Documentation, Wageningen. 189p.

Helmke, P. A. and D. L. Sparks (1996). Lithium, sodium, potassium, rubidium, and cesium. *In* Methods of Soil Analysis. Part 3. Chemical Methods. D. L. Sparks, A. L. Page, P. A. Helmkeet al. Madison, WI, Soil Science Society of America**:** 551-574.

Hillel, D. (1998). Environmental Soil Physics. Academic Press, San Diego. 771p.

Hodnett, M. G. and J. Tomasella (2002). Marked differences between van Genuchten soil water-retention parameters for temperate and tropical soils: new water-retention pedo-transfer functions developed for tropical soils. Geoderma 108: 155-180.

Jipp, P. H., D. C. Nepstad, K. Cassel and C. R. de Carvalho (1998). Deep soil moisture storage and transpiration in forests and pastures of seasonally-dry Amazonia. Climate Change 39: 395-413.

Jordan, C. F. (1982). The nutrient balance of an Amazonian rain forest. Ecology 63(3): 647-654.

Jordan, C. F. and J. Heuveldop (1981). The water budget of an Amazonian rain forest. Acta Amazonica 11: 87-92.

Klinge, R., J. Schmidt and H. Folster (2001). Simulation of water drainage of a rain forest and forest conversion plots using a soil water model. Journal of Hydrology 246: 82-95.

Klute, A. and C. Dirksen (1986). Hydraulic conductivity and diffusivity: laboratory methods. *In* Methods of Soil Analysis, Part 1, Physical and Mineralogical Methods. A. Klute. Madison, Soil Science Society of America. Agronomy Monograph No. 9: 687-734.

Knight, J. H. (1992). Sensitivity of time domain reflectometry measurements to lateral variations in soil water content. Water Resources Research 28(9): 2345-2352.

Knight, J. H., I. White and S. J. Zegelin (1994). Sampling Volume of TDR Probes Used for Water Content Monitoring. *In* Proceedings from the Symposium on TDR in Environmental, Infrastructure, and Mining Applications. Northwestern University, Evanston, IL. Sept. 7-9, 1994. Special Publication SP 19-94, U.S. Dept. of Interior, Bureau of Mines: 93-104.

Leopoldo, P. R., W. K. Franken and N. Augusto Villa Nova (1995). Real evapotranspiration and transpiration through a tropical rain forest in central Amazonia as estimated by the water balance method. Forest Ecology and Management 73: 185-195.

Likens, G. E. and F. H. Bormann (1995). Biogeochemistry of a Forested Ecosystem. Springer-Verlag, New York. 159p.

Marin, C. T., W. Bouten and J. Sevink (2000). Gross rainfall and its partitioning into throughfall, stemflow and evaporation of intercepted water in four forest ecosystems in western Amazonia. Journal of Hydrology 237: 40-57.

Markewitz, D., E. A. Davidson, P. Moutinho and D. Nepstad (in press). Nutrient loss and redistribution after forest clearing on a highly weathered soil in Amazonia. Ecological Applications.

Moreira, M., L. d. S. L. Sternberg and D. C. Nepstad (2000). Vertical patterns of soil water uptake by plants in a primary forest and abandoned pasture in the eastern Amazon: an isotopic approach. Plant and Soil 222: 95-107.

Mualem, Y. (1976). A new model for predicting the hydraulic conductivity of unsaturated porous media. Water Resources Research 12(3): 513-522.

Muller, C. (1999). Modelling Soil-Biosphere Interactions. CABI Publishing, Cambridge, UK. 354p.

Nepstad, D. C., P. Moutinho, M. B. Dias-Filho, E. Davidson, G. Cardinot, D. Markewitz, R. Figueiredo, N. Vianna, J. Chambers, D. Ray, J. B. Guerreiros, P. Lefebvre, L. Sternberg, M. Moreira, L. Barros, F. Y. Ishida, I. Tohlver, E. Belk, K. Kalif and K. Schwalbe (2002). The effects of partial throughfall exclusion on canopy processes, aboveground production, and biogeochemistry of an Amazon forest. Journal of Geophysical Research 107(D20): 8085, doi: 10.1029/2001JD000360.

Nepstad, D. C., C. Uhl, C. A. Pereira and J. M. C. da Silva (1996). A comparative study of tree establishment in abandoned pasture and mature forest of eastern Amazon. Oikos 76: 25-39.

Parton, W. J., D. S. Schimel, C. V. Cole and D. S. Ojima (1987). Analysis of factors controlling soil organic matter levels in Great Plains grasslands. Soil Science Society of America Journal 51: 1173-1179.

Paul, E. A. and F. E. Clark (1996). Soil Microbiology and Biochemistry. Academic Press, San Diego. 340p.

Rasmussen, T. C., R. H. Baldwin, J. F. Dowd and A. G. Williams (2000). Tracer vs. pressure wave velocities through unsaturated saprolite. Soil Science Society of America Journal 64(1): 75-85.

Ribeiro, M. d. N. G. and N. A. Villa Nova (1979). Estudo climatológico da Rreserva Florestal Ducke. III. Evapotranspiração. Acta Amazonica 9: 305-309.

Rocha, H. R. d., P. J. Sellers, G. J. Collatz, I. Wright and J. Grace (1996). Calibration and use of the SiB2 model to estimate water vapour and carbon exchange at the ABRACOS forest sites. *In* Amazonian Deforestation and Climate. J. H. C. Gash, C. A. Nobre, J. M. Roberts and R. L. Victoria. John Wiley and Sons, New York**:** 459-471.

Salati, E. and P. B. Vose (1984). Amazon basin- a system in equilibrium. Science 225(4658): 129-138.

Schlesinger, W. H. (1997). Biogeochemistry: An Analysis of Global Change. Academic Press, New York. 588p.

Sheppard, M. I. and D. H. Thibault (1990). Default soil solid/liquid partition coefficients, $K_d$s, for four major soil types: a compendium. Health Physics 59(4): 471-482.

Shuttleworth, W. J. (1988). Evaporation from Amazonian rain forest. Proceedings of the Royal Society of London Series B. 233(1272): 321-346.

SoilMoisture Equipment Corporation (1986). Guelph Permeameter 2800K1 Operating Instructions. Santa Barbara, CA.

Sternberg, L. d. S. L., M. Moreira and D. C. Nepstad (2002). Uptake of water by lateral roots of small trees in an Amazonian tropical forest. Plant and Soil 238: 151-158.

Thornthwaite, C. W. (1948). An approach toward a rational classification of climate. Geographic Review 38: 55-94.

Thornthwaite, C. W. and J. R. Mather (1957). Instructions and Tables for Computing Potential Evapotranspiration and the Water Balance. Centerton, New Jersey, Drexel Institute of Technology Laboratory of Climatology**:** 311p.

Tomasella, J. and M. G. Hodnett (1998). Estimating soil water retention characteristics from limited data in Brazilian Amazon. Soil Science 163(3): 190-202.

Topp, G. C., J. L. Davis and A. P. Annan (1980). Electromagnetic Determination of Soil Water Content: Measurements in Coaxial Transmission Lines. Water Resources Research 16(3): 574-582.

Ubarana, V. N. (1996). Observations and modelling of rainfall interception at two experimental sites in Amazonia. *in* Amazonian Deforestation and Climate. J. H. C. Gash, C. A. Nobre, J. M. Roberts and R. L. Victoria. John Wiley and Sons, New York**:** 151-162.

van Genuchten, M. T. (1980). A closed-form equation for predicting the hydraulic conductivity of unsaturated soils. Soil Science Society of America Journal 44: 892-898.

Villa Nova, N. A., E. Salati and E. Matsui (1976). Evapotransiração na bacia Amazônica. Acta Amazonica 6: 215-228.

Whittaker, R. H. and G. E. Likens (1973). Carbon in the biota. *In* Carbon and the Biosphere. G. M. Woodwell and E. V. Pecan. National Technical Information Service, Washington, D.C.**:** 281-302.

Wraith, J. M., S. D. Comfort, B. L. Woodbury and W. P. Inskeep (1993). A Simplified Waveform Analysis Approach for Monitoring Solute Transport Using Time-Domain Reflectometry. Soil Science society of America Journal 57: 637-642.

Zegelin, S. J., I. White and D. R. Jenkins (1989). Improved field probes for soil water content and electrical conductivity measurement using Time Domain Reflectometry. Water Resources Research 25(11): 2367-2376.

# CHAPTER 4

# CONCLUSIONS

The darcian method for evaluating unsaturated steady water fluxes predicts measured soil volumetric water contents within 3% water content for the first 960 days of the throughfall exclusion experiment, which includes an 8-month pre-treatment period. As the experiment continues and the vegetation suffers more stress, simplifying assumptions of the model may limit its ability to fully capture the responses. One example is the use of a fixed root distribution. The model would benefit from a dynamic root distribution that accounts for growth and death in each layer and that considers root functionality. This would affect the simulated distribution of water and nutrient uptake between layers and would allow for the reintroduction of nutrients to the soil as roots die. A shift to greater root growth at depth is hypothesized during the continued throughfall exclusion.

Other root functions may also affect soil moisture predictions. For example, if roots serve as passive conduits for redistributing water from wetter to drier regions of the soil, the soil water contents may not be predicted well unless this water movement is accounted for directly. Researchers associated with the throughfall exclusion experiment are currently testing whether such hydraulic lift occurs at this site.

Another suggestion for further model development would be to include the processes of leaf shedding and litter accumulation on the forest floor. As older leaves are

shed and new leaf production declines in response to drought stress, leaf area will also decrease. Rainfall partitioning (i.e. the throughfall fraction) and nutrient inputs from both throughfall and litter decay should be related to these mechanisms. As the canopy opens and the sub-canopy climate changes, soil evaporation may also become more significant.

To realistically model adsorption and desorption of cations, the equilibrium partitioning between particle surfaces and soil solution should be determined for this site. Currently the model does not appear to be predicting these exchanges well, which has a large effect on the predicted concentrations and therefore fluxes of nutrients. Competition by other cations for exchange sites may also be important.

The model is very sensitive to the van Genuchten parameters, which are used to translate water contents to potentials and determine the functions for unsaturated water flow. Theoretically, the water retention properties these parameters describe are physical properties of the soil that can be quantified. If the laboratory-generated water retention data are correct, we should be measuring higher volumetric water contents in the field. However, the soil moisture characteristic curves resulting from model calibration are very similar to published curves for the same soil order. The curves also show similarly low plant-available water. Of course, neither measurement technique is free from error, so further research should be done to resolve this discrepancy. Because of stability issues in the model, it is advisable to minimize the effect of spatial heterogeneity by taking many samples at each depth and using the average values.

During the first treatment year, the measured water contents demonstrate and the model predicts mild soil water depletion near the surface. Persistence of the drought lead to more extensive drying of the surface soils and prevented complete recharge of water

stored deeper in the soil. The model also predicts that evapotranspiration declines, and that water and nutrient fluxes are diminished in response to drought. The complex two-way interactions between vegetation and climate and the unique regional hydrology mean that frequent drought induced by global climate change and local land use conversion could be self-reinforcing.